Hindawi
Mathematical Problems in Engineering
Volume 2018, Article ID 9569834, 25 pages
https://doi.org/10.1155/2018/9569834

Research Article

New Trigonometric Basis Possessing Denominator Shape Parameters

Kai Wang and Guicang Zhang

College of Mathematics and Statistics, Northwest Normal University, Lanzhou 730070, China

Correspondence should be addressed to Kai Wang; 616688448@qq.com

Received 30 July 2018; Accepted 27 September 2018; Published 24 October 2018

Academic Editor: Nhon Nguyen-Thanh

Four new trigonometric Bernstein-like bases with two denominator shape parameters (DTB-like basis) are constructed, based on which a kind of trigonometric Bézier-like curve with two denominator shape parameters (DTB-like curves) that are analogous to the cubic Bézier curves is proposed. The corner cutting algorithm for computing the DTB-like curves is given. Any arc of an ellipse or a parabola can be exactly represented by using the DTB-like curves. A new class of trigonometric B-spline-like basis function with two local denominator shape parameters (DT B-spline-like basis) is constructed according to the proposed DTB-like basis. The totally positive property of the DT B-spline-like basis is supported. For different shape parameter values, the associated trigonometric B-spline-like curves with two denominator shape parameters (DT B-spline-like curves) can be C^2 continuous for a non-uniform knot vector. For a special value, the generated curves can be $C^{(2n-1)}$ $(n = 1, 2, 3, \ldots)$ continuous for a uniform knot vector. A kind of trigonometric B-spline-like surfaces with four denominator shape parameters (DT B-spline-like surface) is shown by using the tensor product method, and the associated DT B-spline-like surfaces can be C^2 continuous for a nonuniform knot vector. When given a special value, the related surfaces can be $C^{(2n-1)}$ $(n = 1, 2, 3, \ldots)$ continuous for a uniform knot vector. A new class of trigonometric Bernstein–Bézier-like basis function with three denominator shape parameters (DT BB-like basis) over a triangular domain is also constructed. A de Casteljau-type algorithm is developed for computing the associated trigonometric Bernstein–Bézier-like patch with three denominator shape parameters (DT BB-like patch). The condition for G^1 continuous jointing two DT BB-like patches over the triangular domain is deduced.

1. Introduction

The construction of basis functions has always been a difficulty of computer-aided geometric design (CAGD). A class of practical basis functions often plays a decisive role in the geometric industry. Conventional cubic B-spline curves and surfaces are widely applied for CAGD due to their remarkable local adjustment properties. However, given control points keep a generated conventional cubic B-spline curve over a single location. Although cubic rational B-spline curves and surfaces can adjust positions and shapes by changing the weighting factor [1–3], their adjustment effect is difficult to predict due to its own defects. In recent years, trigonometric polynomials and splines with one or more shape parameters have been widely used with CAGD, especially in the design of curves and surfaces. Details can be found in [4–7] and the corresponding references therein. For example, researchers have used shape parameters to propose quadratic and cubic trigonometric polynomial splines [8, 9]. In [10], the extended cubic trigonometric spline curve of [8] was given. In [11], a class of C-Bézier curves was constructed in the space span $\{1, t, \sin t, \cos t\}$, where the length of the interval serves as shape parameter. The sine and ellipse curves can be represented by the C-Bézier curves.

Many basis functions with tension effect, which possess one or more parameters, have been proposed to predictably adjust the positions and shapes of generated curves. For example, Nieson [12] proposed a cubic rational spline curve that can generate an interactive curve. The proposed curve can be G^2 continuous with different tension parameters. Barsky [13, 14] provided a class of beta-splines that can locally modify the shape of the generated curves. In a special case, the curve proposed by Barsky contains a kind of uniform B-spline. In [15], Gregory proposed a class of cubic C^2

continuous rational spline, which possesses tension shape parameters so that the shape of the generated curve can be modified. A class of $C^2 \cap FC^3$ spline curves was proposed in [16] by using tension shape parameters. According to [17] and the related references therein, curve design has attracted widespread interest due to the appearance of plenty of exponential splines. In the space $span\{1, t, (1-t)^p, t^q\}$, Costantini constructed a kind of C^2 continuous polynomial splines [18]. In [19, 20], this space was reported to be a quasi-extended Chebyshev space. In [21–25], different points of view about variable degree spaces were proposed. In [26], a class of $\alpha\beta$-Bernstein-like basis was proposed in the space span $\{1, 3t^2 - 2t^3, (1-t)^\alpha, t^\beta\}$. In the space span $\{1, \sin^2, (1 - \sin t)^\alpha, (1 - \cos t)^\beta\}$, four trigonometric Bernstein-like basis functions were constructed [27]. In the space span$\{1, t, (1 - t)^3/[1 + (\alpha - 3)t(1-t)], t^3/[1 + (\beta - 3)t(1-t)\}$, researchers in [28–30] discussed the subdivision scheme with respect to a constructed class of basis functions. In the space span $\{1, 3t^2 - 2t^3, (1-t)^3/[1 + (\alpha - 3)t], t^3/[1 + (\beta - 3)(1-t)]\}$, a cubic rational basis was constructed [31]. In [32, 33], variable degree polynomial splines exhibited enormous potential in the geometric industry in view of the problem of shape preservation and approximation.

Although many improved methods are available, they are rarely applied in solving practical problems. In the final analysis, these techniques increase the flexibility of the curve by adding shape parameters compared with the traditional Bézier and B-spline methods. However, the technique itself cannot replace the traditional method, and several aspects still need improvement. For example, the majority of these methods discuss only basic properties, such as nonnegativity, partition of unity, symmetry, and linear independence. Shape preservation, total positivity, and variation diminishing, which are important properties for curve design, are often overlooked. However, the basis function, which has total positivity, ensures that the related curve contains variation diminishing and shape preservation. Therefore, possessing total positivity is highly important for basis functions. In addition, constructing cubic curves and surfaces remains the main method among the improved techniques. In general, these improved methods have C^2 continuity, thereby meeting engineering requirements. However, in many practical applications, if the requirement for continuity is high, then these methods are slightly insufficient and often need to increase the number of times the curve is constructed. The B-spline curve and surface are regarded as examples. Notably, the continuity and locality of the curved surface are directly related to the number of times. The more times the curve is constructed, the higher the continuous order, but the locality is poor, and the computational complexity is high. Therefore, sacrificing the local property of its dominant position is necessary to achieve the special requirements of high-order continuity. Therefore, in the construction of curves and surfaces, the importance of meeting high-order continuity without increasing the computational complexity and without affecting its local properties is highlighted.

The traditional surface over rectangular domains, which possesses research and application value, has been widely used in CAGD. Obtaining a surface over a rectangular domain is easy because the traditional surface over such domain is a direct extension of the traditional Bézier curve by the tensor product method. However, by using the tensor product method, we fail to extend the patch over a triangular domain because it is not a tensor product surface. In many practical applications, surface modeling based on patch construction over triangular domains is important. Thus, the study of patches over triangular domains is of considerable interest. Therefore, the construction of a practical method that generates patches is important. For this reason, researchers have conducted numerous works. In [34], Cao showed a class of basis functions over a triangular domain. The related patch can be rendered flexible by an adjustment of the values. In [35], Han proposed a patch over a triangular domain, which can construct boundaries that can exactly represent elliptic arcs. A kind of quasi-Bernstein–Bézier polynomials over a triangular domain was proposed in [36]. Recently, Zhu constructed the $\alpha\beta\gamma$-Bernstein–Bézier-like basis, which possesses 10 functions; the related exponential parameter has tension effect.

This study proposes a class of DTB-like bases with tension effects that is based on previous studies. The proposed basis has two denominator shape parameters constructed in the space $span\{1, \sin^2 t, (1 - \sin t)^2/[1 + (\alpha - 2)\sin t], (1 - \cos t)^2/[1 + (\beta - 2)\cos t]\}$ and can form an optimal normal normalized totally positive basis (B-basis) and a new class of DT BB-like basis functions over a triangular domain with three denominator shape parameters. The presented DT B-spline-like curves and surfaces are C^2 continuous with respect to a nonuniform knot vector. The corresponding curves and surfaces are C^{2n-1} $(n = 1, 2, \ldots)$ continuous for the shape parameters, which select a special value with respect to a uniform knot vector. The denominator parameter introduced in the basis function has a tension effect, and the parameters can be used to predictably adjust the corresponding curves and surfaces generated.

The remainder of this work is organized as follows. Section 2 provides the definition and properties of the DTB-like basis functions and shows the corresponding curves. Section 3 presents a class of DT B-spline-like basis with two denominator shape parameters. The properties of the proposed basis are analyzed, and the associated DT B-like curves are shown. Section 4 proposes a class of DT BB-like basis over a trigonometric domain with three denominator shape parameters. We provided the definition and properties of related DT BB-like patches on the basis of the presented basis functions. Then, we developed a de Casteljau algorithm to calculate the proposed patch. Finally, G^1 connecting conditions of the two proposed patches are given. Section 5 presents the conclusion.

2. Trigonometric Bernstein-Like Basis Functions

2.1. Preliminaries. For a good understanding of this study, related background knowledge about the extended Chebyshev (EC) space and the extended completed Chebyshev

(ECC) space is provided in this subsection. Additional details are available in [37–39].

$a < b$ for any closed bounded interval $[a,b]$, which can be denoted by I. The function space $(u_0,\dots,u_n)$ is called $n+1$-dimension ECC-space, which is generated by the positive weight function $w_j \in C^{n-j}(I)$ in canonical form. The weight function shows that

$$\begin{aligned} u_0(t) &= w_0(t), \\ u_1(t) &= w_0(t)\int_a^t w_1(t_1)\,dt_1, \\ u_2(t) &= w_0(t)\int_a^t w_1(t_1)\int_a^{t_1} w_2(t_2)\,dt_2 dt_1, \\ &\vdots \\ u_n(t) &= w_0(t) \\ &\quad\cdot\int_a^t w_1(t_1)\int_a^{t_1} w_2(t_2)\cdots\int_a^{t_{n-1}} w_n(t_n)\,dt_n\cdots dt_1. \end{aligned} \tag{1}$$

The necessary and sufficient condition of $n+1$-dimension function space $(u_0,\dots,u_n)\subset C^n(I)$ is called an ECC-space on I that is for arbitrary k, $0\le k\le n$, and an arbitrary nontrivial linear combination of the elements of the subspace $(u_0,\dots,u_k)$ with the most k zeros (counting multiplicities).

If the collocation matrix $(u_j(t_i))_{0\le i,j\le n}$ related to the basis $(u_0,\dots,u_n)$ for an arbitrary sequence of points $a\le t_0<t_1<\cdots<t_n\le b$ is totally positive, then the basis is deemed totally positive on $[a,b]$. If a function space has a totally positive basis, then the other totally positive basis can be formed by multiplying the optimal normalized totally positive basis (B-basis) by a totally positive matrix. Moreover, this basis is unique in space and has optimal shape preservation properties [40–42].

Assume that $n+1$-dimensional $\varepsilon\subset C^n$ is an $n+1$-dimensional EC-space on closed bounded interval I, which possesses constants, where $n\ge 2$. Select n functions $\Phi_1,\dots,\Phi_n$ in ε so that $(1,\Phi_1,\dots,\Phi_n)$ forms a basis of ε. We set a mother function $\Phi := (1,\Phi_1,\dots,\Phi_n): I\longrightarrow R^n$. This function being C^n on I, for arbitrary nonnegative integer $i\le n-1$, we can consider its osculating flat of order i at $x\in I$, defined as the affine space passing through $\Phi(x)$ and the direction of which is spanned by $\Phi'(x),\dots,\Phi^{(i)}(x)$, that is,

$$\begin{aligned} Osc_i\Phi(x) := \{&\Phi(x)+\lambda_1\Phi'(x)+\cdots \\ &+\lambda_i\Phi^{(i)}(x)\mid \lambda_1,\dots\lambda_i\in R\}. \end{aligned} \tag{2}$$

For arbitrary positive integers $\mu_1,\dots,\mu_r$, with $\sum_{i=1}^r\mu_i=n$, and arbitrary pairwise distinct $a_1,\dots,a_r$ in I, if ever the r osculating flats $Osc_{n-\mu_i}\Phi(a_i)$, $1\le i\le r$, possess a unique common point, then we define the blossom of Φ as the function $\varphi := (\varphi_1,\dots\varphi_n): I^n\longrightarrow R^n$ such that

$$\{\varphi(x_1,\dots,x_n)\} := \bigcap_{i=0}^{n} Osc_{n-\mu_i}\Phi(a_i). \tag{3}$$

The arbitrary n-tuple $(x_1,\dots,x_n)$ is equivalent to $(a_1^{[\mu_1]},\dots,a_1^{[\mu_n]})$ up to permutation, where

$$\left(a_1^{[\mu_1]},\dots,a_r^{[\mu_r]}\right) := \left(\underbrace{a_1,\dots,a_1}_{\mu_1},\dots\underbrace{a_1,\dots,a_1}_{\mu_r}\right). \tag{4}$$

Reference [37] showed that the blossom that exists in space ε deduces three important properties, namely, pseudo-affinity, diagonal, and symmetry. In addition, we must emphasize a useful conclusion that the blossom that exists in space ε is equal to that in space $D\varepsilon$, which is an EC- space on I. Additional details can be seen in Theorem 3.1 in [38].

For arbitrary $(a,b)\in I^2$, the $n+1$ points $P_i(a,b) := \varphi(a^{[n-i]},b^{[i]})$, $i=0,\dots,n$, are defined by the Chebyshev–Bézier points of φ about (a,b). When $a=b$, $P_i(a,b)=\varphi(a)$, for all $i=0,\dots,n$. However, when $a\ne b$, the Chebyshev–Bézier points are obtained as

$$\begin{aligned} &\Pi_0(a,b)=\Phi(a), \\ &\Pi_n(a,b)=\Phi(b), \\ &\{\Pi_i(a,b)\}=Osc_i\Phi(a)\cap Osc_{n-i}\Phi(b),\quad 1\le i\le n-1. \end{aligned} \tag{5}$$

Moreover, when $a\ne b$, a de Casteljau algorithm starting from points $\Pi_i(a,b)$ can be developed by using the three important properties of the blossom. At the nth step of this algorithm, the values of φ can be obtained as

$$\begin{aligned} &\Phi(x)=\sum_{i=0}^{n} B_i^{(a,b)}(x)\,\Pi_i(a,b), \\ &\sum_{i=0}^{n} B_i^{(a,b)}(x)=1, \\ &\qquad\qquad x\in I. \end{aligned} \tag{6}$$

Given that $(1,\Phi_1,\dots,\Phi_n)$ is a set of bases in the function of ε, the affine flat of the mother function Φ spans the whole space R^n. Therefore, points $\Pi_0(a,b),\dots,\Pi_n(a,b)$ are affinely independent. Furthermore, $B_i^{(a,b)}$, $i=0,\dots,n$, from a basis of ε [37].

2.2. Construction of Trigonometric Basis Function. For arbitrary real numbers $\alpha,\beta\in[2,+\infty)$, $t\in[0,\pi/2]$, we consider constructing a basis function in the trigonometric function space $T_{\alpha,\beta} := span\{1,\sin^2 t,(1-\sin t)^2/(1+(\alpha-2)\sin t),(1-\cos t)^2/(1+(\beta-2)\cos t)\}$. We can easily obtain the corresponding mother function, which is defined as

$$\begin{aligned} &\Phi(t) := \left\{\sin^2 t,\frac{(1-\sin t)^2}{1+(\alpha-2)\sin t},\frac{(1-\cos t)^2}{1+(\beta-2)\cos t}\right\}, \\ &\qquad\qquad t\in\left[0,\frac{\pi}{2}\right]. \end{aligned} \tag{7}$$

First, let us prove that the space

$$DT_{\alpha,\beta} = span\left\{2\sin t\cos t, -\frac{\cos t\,(1-\sin t)\,[\alpha+(\alpha-2)\sin t]}{[1+(\alpha-2)\sin t]^2}, \frac{\sin t\,(1-\cos t)\,[\beta+(\beta-2)\cos t]}{[1+(\beta-2)\cos t]^2}\right\} \tag{8}$$

is a three-dimensional EC-space on $[0,\pi/2]$. Therefore, according to Theorem 2.1 of [38], $T_{\alpha,\beta}$ possesses a blossom, indicating that $T_{\alpha,\beta}$ is suitable for curve and surface designs.

Theorem 1. *For arbitrary real numbers $\alpha,\beta\in[2,+\infty)$, $DT_{\alpha,\beta}$ is a three-dimensional EC-space on $[0,\pi/2]$.*

Proof. For arbitrary $\xi_i\in R$ $(i=0,1,2)$, $t\in[0,\pi/2]$, we consider a linear combination

$$\xi_0[2\sin t\cos t] + \xi_1\left\{-\frac{\cos t\,(1-\sin t)\,[\alpha+(\alpha-2)\sin t]}{[1+(\alpha-2)\sin t]^2}\right\} + \xi_2\left\{\frac{\sin t\,(1-\cos t)\,[\beta+(\beta-2)\cos t]}{[1+(\beta-2)\cos t]^2}\right\} = 0. \tag{9}$$

For $t=0$, from (9), we can easily obtain $\xi_1=0$. In the same way, for $t=\pi/2$, from (9), we can obtain $\xi_2=0$. Thus, $\xi_0=0$. Therefore, $DT_{\alpha,\beta}$ is a three-dimensional space.

Below, we prove that $DT_{\alpha,\beta}$ is an ECC-space in $[0,\pi/2]$. For arbitrary $t\in[a,b]\subseteq(0,\pi/2)$, let

$$u(t) = \left\{-\frac{(1-\sin t)\,[\alpha+(\alpha-2)\sin t]}{\sin t\,[1+(\alpha-2)\sin t]^2}\right\}' = \cos t\cdot\frac{\left[3\sin t\,(2-\sin t)+1+(\alpha-2)\left(3-\sin^2 t\right)\sin t\right](\alpha-2)+2}{\sin^2 t\,[1+(\alpha-2)\sin t]^3} > 0 \tag{10}$$

and

$$v(t) = \left\{\frac{(1-\cos t)\,[\beta+(\beta-2)\cos t]}{[1+(\beta-2)\cos t]^2}\right\}' = \sin t\cdot\frac{\left[3\cos t\,(2-\cos t)+1+(\beta-2)\left(3-\cos^2 t\right)\cos t\right](\beta-2)+2}{\cos^2 t\,[1+(\beta-2)\cos t]^3} > 0. \tag{11}$$

Direct computation indicates that

$$u'(t) = -\sin t\frac{\left[3\sin t\,(2-\sin t)+1+(\alpha-2)\left(3-\sin^2 t\right)\sin t\right](\alpha-2)+2}{\sin^2 t\,[1+(\alpha-2)\sin t]^3} - 2\cos^2 t\cdot\frac{2+(\alpha-2)(1+8\sin t)+(\alpha-2)^3\sin^2 t\,[5+(1+\sin t)(1-\sin t)]+4(\alpha-2)^2\sin t\,[(2-\sin t)\sin t+\sin t+1]}{\sin^3 t\,[1+(\alpha-2)\sin t]^4} < 0, \tag{12}$$

$$v'(t) = \sin t\frac{\left[3\cos t\,(2-\cos t)+1+(\beta-2)\left(3-\cos^2 t\right)\cos t\right](\beta-2)+2}{\cos^2 t\,[1+(\beta-2)\cos t]^3} + \sin^2 t\cdot\frac{2+(\beta-2)(1+8\cos t)+(\beta-2)^3\cos^3 t\,[5+(1+\cos t)(1-\cos t)]+4(\beta-2)^2\cos t\,[(2-\cos t)\cos t+\cos t+1]}{\cos^3 t\,[1+(\beta-2)\cos t]^4} > 0. \tag{13}$$

Thus, for the Wronskian of $u(t)$ and $v(t)$,

$$W(u,v)(t) = u(t)\,v'(t) - u'(t)\,v(t) > 0,\quad \forall t\in\left[0,\frac{\pi}{2}\right]. \tag{14}$$

For $t\in[a,b]$, we obtain the definition of the following weight functions:

$$\omega_0(t) = 2\sin t\cos t,$$

$$\omega_1(t) = Au(t) + Bv(t),$$

$$\omega_2(t) = C\frac{W(u,v)(t)}{[Au(t)+Bv(t)]^2}, \tag{15}$$

where A,B,C are three arbitrary positive real numbers. All of the three weight functions $\omega_i(t)$ $(i=0,1,2)$ are bounded, positive, and C^∞ on closed bounded $[a,b]$. Next, we discuss the following ECC-spaces:

$$u_0(t) = \omega_0(t),$$

$$u_1(t) = \omega_0(t)\int_a^t \omega_1(t_1)\,dt_1,$$

$$u_2(t) = \omega_0(t) \int_a^t \omega_1(t_1) \int_a^{t_1} \omega_2(t_2)\, dt_2 dt_1, \tag{16}$$

We can easily verify that these functions $u_i(t)$ $(i = 0, 1, 2)$ are linear combinations of

$$2\sin t\cos t, -\frac{\cos t(1-\sin t)[\alpha + (\alpha-2)\sin t]}{[1+(\alpha-2)\sin t]^2}, \\ \frac{\sin t(1-\cos t)[\beta + (\beta-2)\cos t]}{[1+(\beta-2)\cos t]^2}. \tag{17}$$

Thus, $DT_{\alpha,\beta}$ is an ECC-space on $[a, b]$. Furthermore, $[a, b]$ are any subintervals of $(0, \pi/2)$; hence, $DT_{\alpha,\beta}$ is also an ECC-space on $(0, \pi/2)$.

Proof that $DT_{\alpha,\beta}$ is an EC-space on $[0, \pi/2]$ is provided. Thus, we must verify that the arbitrary nonzero element of $DT_{\alpha,\beta}$ has, at most, two zeros (counting multiplicities) on $[0, \pi/2]$.

Consider the arbitrary nonzero function

$$G(t) = C_0[2\sin t\cos t] \\ + C_1\left\{-\frac{\cos t(1-\sin t)[\alpha + (\alpha-2)\sin t]}{[1+(\alpha-2)\sin t]^2}\right\} \\ + C_2\left\{\frac{\sin t(1-\cos t)[\beta + (\beta-2)\cos t]}{[1+(\beta-2)\cos t]^2}\right\}, \tag{18}$$

where $t \in [0, \pi/2]$. $G(t)$ has, at most, two zeros in $(0, \pi/2)$ because $DT_{\alpha,\beta}$ is an ECC-space in $(0, \pi/2)$. Initially, $G(t)$ is assumed to vanish at 0; then, we can obtain $C_1 = 0$. Under these circumstances, if $C_2 = 0$, then $G(t)$ has two singular zeros at 0 and $\pi/2$. If $C_0 = 0$, then 0 is a double zero of $G(t)$. If $C_0C_2 > 0$, then $G(t)$ has a singular zero at 0 but does not have a zero on $(0, \pi/2]$. If $C_0C_2 < 0$, then $G(t)$ has a singular zero at 0 but not at $\pi/2$. In addition, for the function,

$$K(t) \coloneqq 2C_0\cos t + C_2\frac{(1-\cos t)[\beta + (\beta-2)\cos t]}{[1+(\beta-2)\cos t]^2}, \tag{19}$$

direct computation yields

$$K'(t) = -2C_0\cos t + C_2\frac{2(b-1)^2\sin t}{[1+(b-2)\cos t]^3}, \tag{20}$$

where $K(t)$ is a monotonic function on $[0, \pi/2]$. From these values, together with $K(0)K(\pi/2) = 2\beta C_0C_2 < 0$, we can see that $K(t)$ has exactly one zero in $(0, \pi/2)$. Thus, we can immediately conclude that $G(t) = \sin tK(t)$ has one zero in $(0, \pi/2)$. Similarly, if $G(t)$ vanishes at $\pi/2$, then function $G(t)$ has, at most, two zeros on $[0, \pi/2]$ (counting multiplicities as far as possible up to 2). In summary, the space $DT_{\alpha,\beta}$ is an EC-space on $[0, \pi/2]$.

Therefore, $DT_{\alpha,\beta}$ is an EC-space on $[0, \pi/2]$. According to Theorem 3.1 in [43], a blossom exists in $T_{\alpha,\beta}$. This theorem also means that $T_{\alpha,\beta}$ is suitable for curve and surface designs. According to Theorem 2.18 in [43], we can also infer that $T_{\alpha,\beta}$ has a B-basis on $[0, \pi/2]$. □

Theorem 2. *The four Chebyshev–Bézier points $P_i \coloneqq P_i(0, \pi/2)$ of the mother function $\Phi(t)$ defined in (7) are given by*

$$\Pi_0 = (0, 1, 0), \\ \Pi_1 = (0, 0, 0), \\ \Pi_0 = (1, 0, 0), \\ \Pi_0 = (1, 0, 1). \tag{21}$$

Moreover, the related new cubic trigonometric Bernstein-like basis $A_i \coloneqq A_i^{(0,\pi/2)}$ of $T_{\alpha,\beta}$ are given by

$$A_0(t) = \frac{(1-\sin t)^2}{1+(\alpha-2)\sin t}, \\ A_1(t) = 1 - \sin^2 t - \frac{(1-\sin t)^2}{1+(\alpha-2)\sin t}, \\ A_2(t) = 1 - \cos^2 t - \frac{(1-\cos t)^2}{1+(\beta-2)\cos t}, \\ A_3(t) = \frac{(1-\cos t)^2}{1+(\beta-2)\cos t}. \tag{22}$$

Proof. Through the definition of $\Phi(t)$ given in (7), we can easily obtain

$$\Phi(0) = (0, 1, 0), \\ \Phi\left(\frac{\pi}{2}\right) = (1, 0, 1), \\ \Phi'(0) = (0, -\alpha, 0), \\ \Phi'\left(\frac{\pi}{2}\right) = (0, 0, \beta), \\ \Phi''(0) = \left(2, 2(\alpha-1)^2, 0\right), \\ \Phi''\left(\frac{\pi}{2}\right) = \left(-2, 0, 2(\beta-1)^2\right). \tag{23}$$

Thus, by simply computing, we have

$$\Pi_0 = \Phi(0) = (0, 1, 0), \\ \Pi_3 = \Phi\left(\frac{\pi}{2}\right) = (1, 0, 1), \\ \{\Pi_1\} = Osc_1\Phi(0) \cap Osc_2\Phi\left(\frac{\pi}{2}\right) = (0, 0, 0), \\ \{\Pi_2\} = Osc_2\Phi(0) \cap Osc_1\Phi\left(\frac{\pi}{2}\right) = (1, 0, 0). \tag{24}$$

Thus, for any $t \in [0, \pi/2]$, from $\Phi(t) = \sum_{i=0}^{3} A_i(t)\Pi_i$ together with $\sum_{i=0}^{3} A_i(t) = 1$, we obtain the expressions of $A_i(t)$, $i = 0, 1, 2, 3$. □

Remark 3. From the expressions of the basis function given in (22), we can infer that (22) has important properties, such as

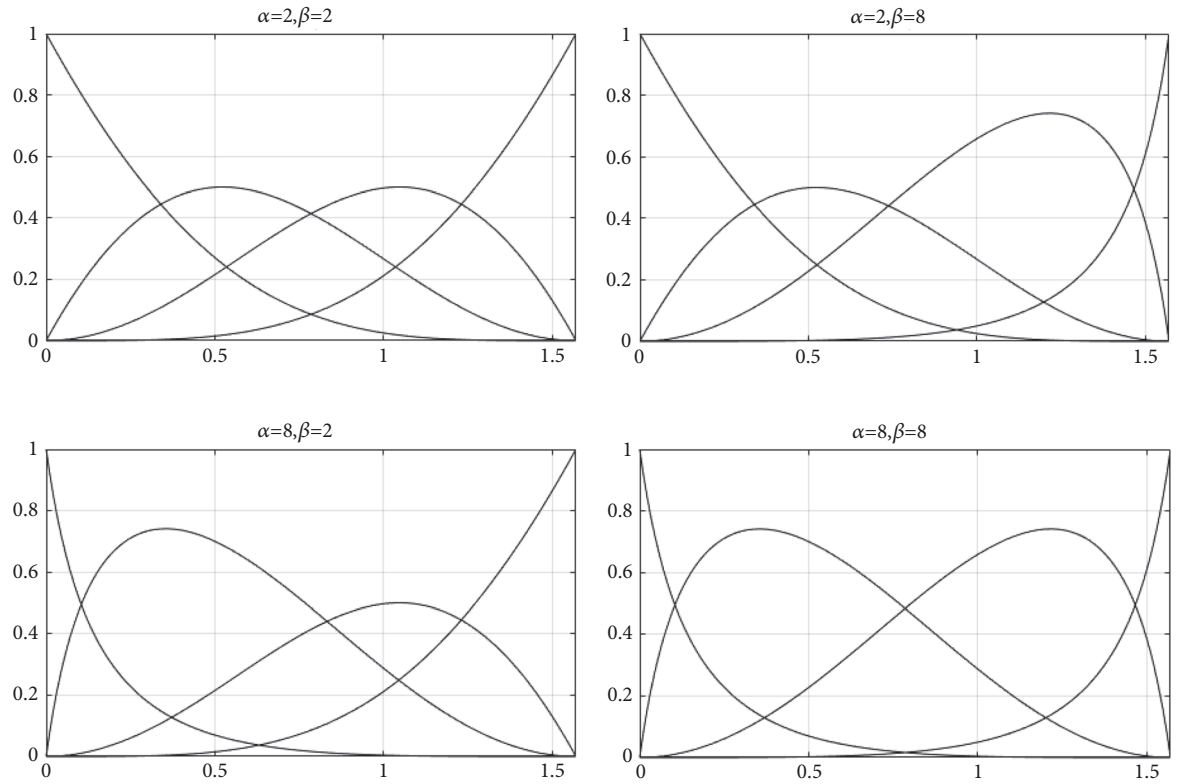

Figure 1: DTB-like basis under different shape parameters.

linear independence, nonnegativity, and partition of unity. In addition, for all $i = 0, 1, 2, 3$, we have the following end-point properties:

$$A_i^{(j)}(0) = 0, \quad j = 0, \ldots, i-1,$$
$$A_i^{(i)}(0) > 0, \tag{25}$$
$$A_i^{(j)}\left(\frac{\pi}{2}\right) = 0, \quad j = 0, \ldots, 2-i.$$

Thus, system $(A_0(t), A_1(t), A_2(t), A_3(t))$ is precisely the B-basis of $T_{\alpha,\beta}$, which implies that (22) possesses totally positive and optimal shape preservation properties [33].

We define a cubic trigonometric Bernstein-like basis with denominator shape parameters given in (22) as $A_i(t;\alpha,\beta)$, $i = 0, 1, 2, 3$, or $A_i(t;\alpha)$, $i = 0, 1$ and $A_i(t;\beta)$, $i = 2, 3$ to facilitate the following discussion and distinguish the traditional literature. Figure 1 shows images of the DTB-like basis under different shape parameters.

2.3. DTB-Like Curve with Denominator Shape Parameters

Definition 4. Given control points P_i $(i = 0, 1, 2, 3)$ in R^2 or R^3,

$$Q(t;\alpha,\beta) = \sum_{i=0}^{3} A_i(t;\alpha,\beta) P_i, \quad t \in \left[0, \frac{\pi}{2}\right], \ \alpha, \beta \in [2, +\infty), \tag{26}$$

are called a cubic DTB-like curve with two denominator shape parameters α and β.

Thus, the corresponding DTB-like curve given in (26) has the properties of affine invariance, convex hull, and variation diminishing, which are crucial properties in curve design, given that (22) possesses the properties of partition of unity, nonnegativity, and total positivity. Moreover, we have the following end-point property:

$$\begin{aligned} Q(0;\alpha,\beta) &= P_0, \\ Q\left(\frac{\pi}{2};\alpha,\beta\right) &= P_3, \\ Q'(0;\alpha,\beta) &= \alpha(P_1 - P_0), \\ Q'\left(\frac{\pi}{2};\alpha,\beta\right) &= \beta(P_3 - P_2), \\ Q''(0;\alpha,\beta) &= 2(\alpha-1)^2(P_0 - P_1) + 2(P_2 - P_1), \\ Q''\left(\frac{\pi}{2};\alpha,\beta\right) &= 2(\beta-1)^2(P_3 - P_2) + 2(P_1 - P_2). \end{aligned} \tag{27}$$

For arbitrary $\alpha, \beta \in [2, +\infty)$, the curve given in (26) has the end-point interpolation property, and P_0P_1 and P_2P_3 are the tangent lines of the curve at points P_0 and P_3, respectively. From these properties, we can easily find that the curve given in (26) has similar geometric properties to the classical cubic Bézier curve.

The corner cutting algorithm is a steady and high-efficiency algorithm for generating the presented DTB-like curves. We rewrite (26) into the following matrix to develop the algorithm:

$$Q(t;\alpha,\beta) = \left(1-\sin^2 t \quad 1-\cos^2 t\right) \times \begin{pmatrix} 1-\sin t & \sin t & 0 \\ 0 & \cos t & 1-\cos t \end{pmatrix} \times \begin{pmatrix} \frac{1}{(1+\sin t)[1+(\alpha-2)\sin t]} & \frac{(1+\sin t)[1+(\alpha-2)\sin t]-1}{(1+\sin t)[1+(\alpha-2)\sin t]} \\ 0 & \frac{\cos t}{\sin t+\cos t} \\ 0 & 0 \end{pmatrix} \times \begin{pmatrix} 0 & 0 \\ \frac{\sin t}{\sin t+\cos t} & 0 \\ \frac{(1+\cos t)[1+(\beta-2)\cos t]-1}{(1+\cos t)[1+(\beta-2)\cos t]} & \frac{1}{(1+\cos t)[1+(\beta-2)\cos t]} \end{pmatrix} \times \begin{pmatrix} P_0 \\ P_1 \\ P_2 \\ P_3 \end{pmatrix}. \tag{28}$$

By rewriting the curve expression into matrix form, we can rapidly obtain this algorithm. Figure 2 shows an example of this algorithm.

In addition, for $t \in [0, \pi/2]$, we can rewrite (26) into the following form:

$$Q(t;\alpha,\beta) = \sin^2 P_1 + \cos^2 P_2 + A_0(t;\alpha)(P_0 - P_1) + A_3(t;\beta)(P_3 - P_2). \tag{29}$$

For arbitrary fixed $t \in (0, \pi/2)$, $A_0(t;\alpha)$ monotonically decreases with respect to the shape parameter α. This phenomenon also means that, as shape parameter α increases, the generated curve moves in the same direction as the edge $P_0 - P_1$. By contrast, as shape parameter α decreases, the opposite is true for the generated curve. On the edge $P_3 - P_2$, parameter β has similar influences. When $\alpha = \beta$, as the shape parameters increase or decrease, the generated curve moves to the edge $P_2 - P_1$ in the same or opposite direction, respectively. Thus, the two denominator shape parameters have a tension effect. Figure 3 shows the generated curves for different shape parameter values.

2.4. Representation of Elliptic and Parabolic Arcs. For $\alpha = \beta = 2$, if the control points are $P_0 = (x_0 + a, y_0)$, $P_1 = (x_0 + a, y_0 + b/2)$, $P_2 = (x_0 + a/2, y_0 + b)$, and $P_3 = (x_0, y_0 + b)$, then the coordinates of the generated curve $T(t;2,2)$ are

$$\begin{aligned} x(t) &= x_0 + a\cos t, \\ y(t) &= y_0 + b\sin t, \\ t &\in \left[0, \frac{\pi}{2}\right], \end{aligned} \tag{30}$$

where $T(t;2,2)$ is a quarter of an elliptic arc whose center is located at (x_0, y_0). By constraining the parameter t on the desired interval $[\theta_1, \theta_2]$, we can obtain an arc of an ellipse whose starting and ending angles are θ_1 and θ_2, respectively.

Furthermore, for $\alpha = \beta = 2, b-a > 0$, if the control points P_0, P_1, P_2, and P_3 with respective coordinates $(b, c_2b^2 + c_1b + c_0)$, $(b, c_2b^2 + c_1b + c_0)$, $((a+b)/2, c_2ab + c_1(a+b)/2 + c_0)$, and $(a, c_2a^2 + c_1a + c_0)$, then we obtain the following from (26):

$$\begin{aligned} x(t) &= (b-a)\cos t + a, \\ y(t) &= c_2[(b-a)\cos t + a]^2 + c_1[(b-a)\cos t + a] + c_0, \\ t &\in \left[0, \frac{\pi}{2}\right], \end{aligned} \tag{31}$$

which presents a segment of the parabola $y = c_2x^2 + c_1x + c_0$, $x \in [a, b]$.

The discussion indicates that any arc of an ellipse or parabola can be exactly represented by using the proposed DTB-like curves. Figure 4 shows the elliptic and parabolic segments generated by using the cubic DTB-like curves (marked with solid black lines).

3. DT B-Spline-Like Basis Function

3.1. Construction of Trigonometric B-Spline-Like Basis Functions. Given a sequence of knots $u_0 < u_1 < \cdots < u_{n+4}$, we refer to $U = (u_0, u_1, \ldots, u_{n+4})$ as a knot vector. Let $h_j = u_{j+1} - u_j$, and $t_j(u) = \pi(u - u_j)/2h_j$, $j = 0, 1, \ldots, n+3$, for arbitrary real numbers $\alpha_i, \beta_i \in [2, +\infty)$, $i = 0, 1, \ldots, n$, we construct trigonometric B-spline-like basis functions with the following forms:

$$B_i(u) = \begin{cases} B_{i,0}(t_i) = d_iA_3(t_i;\beta_i), & u \in [u_i, u_{i+1}), \\ B_{i,1}(t_{i+1}) = \sum_{j=0}^{3} c_{i+1,j}A_j(t_{i+1}, \alpha_{i+1}, \beta_{i+1}), & u \in [u_{i+1}, u_{i+2}), \\ B_{i,2}(t_{i+2}) = \sum_{j=0}^{3} b_{i+2,j}A_j(t_{i+2}, \alpha_{i+2}, \beta_{i+2}), & u \in [u_{i+2}, u_{i+3}), \\ B_{i,3}(t_{i+3}) = a_{i+3}A_0(t_{i+3};\alpha_{i+3}), & u \in [u_{i+3}, u_{i+4}), \\ 0, & u \notin [u_i, u_{i+4}), \end{cases} \tag{32}$$

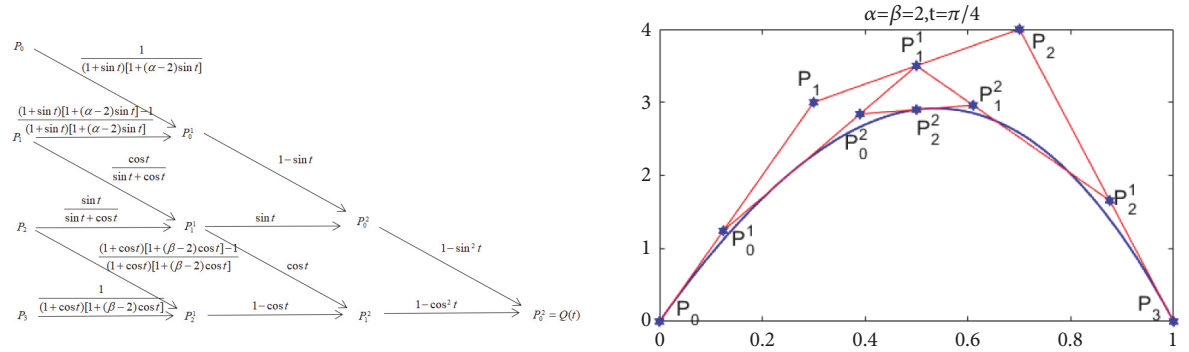

Figure 2: Corner cutting algorithm.

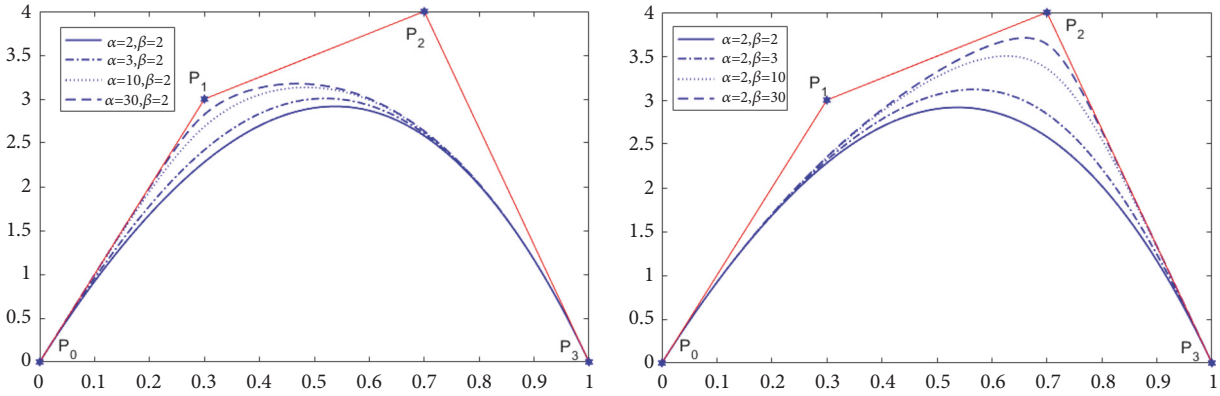

Figure 3: DTB-like curve with different shape parameters.

where $A_j(t_i;\alpha_i,\beta_i)$, $j = 0,1,2,3$ are the DTB-like basis functions given in (22).

To determine $a_i, b_{i,j}, c_{i,j}, d_i$ coefficient values of the basis functions (32), we add two restricting conditions: (1) including C^2 continuity at each knot and (2) forming a partition of unity on $[a,b]$. Direct computation shows that

$$\begin{aligned}
\lambda_i &= (\alpha_{i+1}-1)^2\beta_i h_i + \alpha_{i+1}(\beta_i-1)^2 h_{i+1},\\
\mu_i &= \alpha_{i+1}h_i + \beta_i h_{i+1},\\
\phi_i &= \frac{\lambda_i h_i + \mu_i h_{i+1}}{\beta_i h_{i+1}^2},\\
\varphi_i &= \frac{\lambda_{i-1} h_i + \mu_{i-1} h_{i-1}}{\alpha_i h_{i-1}^2}\\
a_i &= \frac{\beta_{i-1}\lambda_{i-2}h_i^2}{\lambda_{i-1}\mu_{i-2}h_{i-2} + \lambda_{i-2}\lambda_{i-1}h_{i-1} + \lambda_{i-2}\mu_{i-1}h_i},\\
d_i &= \frac{\alpha_{i+1}\lambda_{i+1}h_i^2}{\lambda_{i+1}\mu_i h_i + \lambda_i\lambda_{i+1}h_{i+1} + \lambda_i\mu_{i+1}h_{i+2}},\\
b_{i,0} &= \frac{\alpha_i\phi_i h_{i-1}}{\mu_{i-1}}a_{i+1} + \frac{\beta_{i-1}\varphi_{i-1}h_i}{\mu_{i-1}}d_{i-2},\\
c_{i,0} &= d_{i-1},\\
b_{i,1} &= \phi_i a_{i+1},\\
c_{i,1} &= \frac{\mu_{i-1}}{\alpha_i h_{i-1}}d_{i-1},\\
b_{i,2} &= \frac{\mu_i}{\beta_i h_{i+1}}a_{i+1},\\
c_{i,2} &= \varphi_i d_{i-1},\\
b_{i,3} &= a_{i+1},\\
c_{i,3} &= \frac{\alpha_{i+1}\phi_{i+1}h_i}{\mu_i}a_{i+2} + \frac{\beta_i\varphi_i h_{i+1}}{\mu_i}d_{i-1}.
\end{aligned} \tag{33}$$

We will provide the following definition to facilitate the following discussion and distinguish the traditional literature.

Definition 5. For arbitrary real numbers $\alpha_i, \beta_i \in [2,+\infty)$, given a knot vector U, with the coefficients $a_i, b_{i,j}, c_{i,j}, d_i$, (32) expressions are defined as DT B-spline-like basis with two denominator shape parameters.

Remark 6. The DT B-spline-like basis functions are constructed in the space

$$\begin{aligned}
S := \{ & s \in C^2[u_0, u_{n+4}] \ \ s.t..\ \ s|_{[u_i,u_{i+1}]} \in T_{\alpha_i,\beta_i},\ \alpha_i,\beta_i\\
& \in [2,+\infty),\ i = 0,1,\ldots,n+3\},
\end{aligned} \tag{34}$$

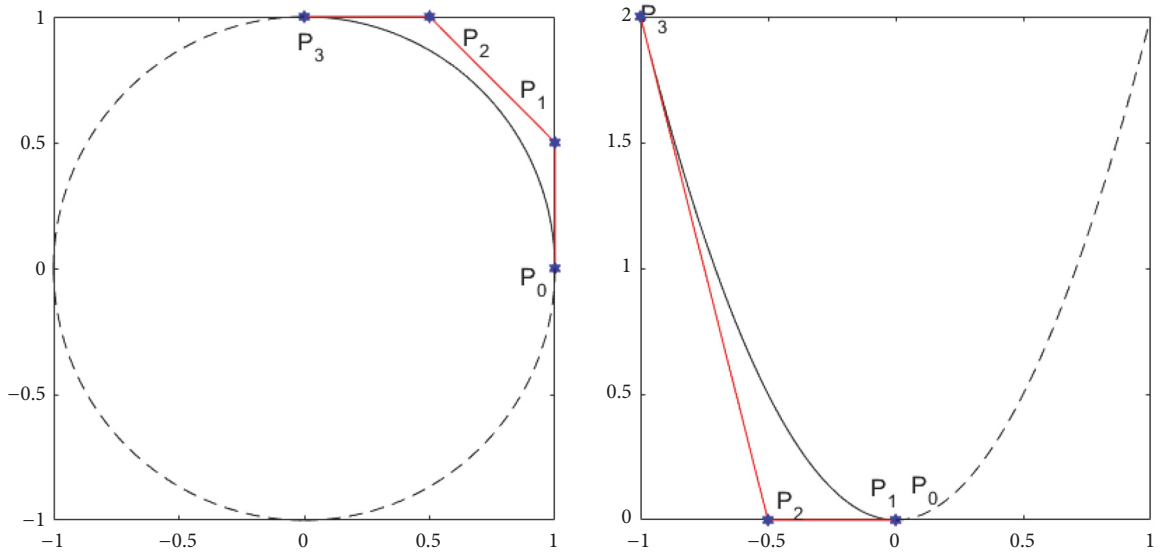

Figure 4: Representation of elliptic and parabolic arcs.

where

$$T_{\alpha_i,\beta_i} := span\left\{1, \sin^2 t, \frac{(1-\sin t)^2}{1+(\alpha_i-2)\sin t}, \frac{(1-\cos t)^2}{1+(\beta_i-2)\cos t}\right\}. \tag{35}$$

In particular, for $u_{i+j} = u_i + jh, h > 0$, $j = 1, 2, 3, 4$ and $\alpha_{i+1} = \alpha_{i+2} = \alpha_{i+3} = \beta_i = \beta_{i+1} = \beta_{i+2} = 2$, direct computation yields

$$\begin{aligned} d_i &= \frac{1}{6}, \\ c_{i+1,0} &= \frac{1}{6}, \\ c_{i+1,1} &= \frac{1}{3}, \\ c_{i+1,2} &= \frac{2}{3}, \\ c_{i+1,3} &= \frac{2}{3}, \\ b_{i+2,0} &= \frac{2}{3}, \\ b_{i+2,1} &= \frac{2}{3}, \\ b_{i+2,2} &= \frac{1}{3}, \\ b_{i+2,3} &= \frac{1}{6}, \\ a_{i+3} &= \frac{1}{6}, \end{aligned} \tag{36}$$

from which we can immediately obtain the following explicit expressions of $B_i(u)$:

$$B_i(u) = \begin{cases} \frac{1}{6}(1-\cos t_i)^2 & u \in [u_i, u_i + h), \\ \frac{1}{6}(1-\sin t_{i+1})^2 + \frac{1}{3}[2\sin t_{i+1}(1-\sin t_{i+1})] & \\ \quad + \frac{2}{3}[2\cos t_{i+1}(1-\cos t_{i+1})] + \frac{2}{3}(1-\sin t_{i+1})^2 & u \in [u_i + h, u_i + 2h), \\ \frac{2}{3}(1-\sin t_{i+2})^2 + \frac{2}{3}[2\sin t_{i+2}(1-\sin t_{i+2})] & \\ \quad + \frac{1}{3}[2\cos t_{i+2}(1-\cos t_{i+2})] + \frac{1}{6}(1-\sin t_{i+2})^2 & u \in [u_i + 2h, u_i + 3h), \\ \frac{1}{6}(1-\sin t_{i+3})^2 & u \in [u_i + 3h, u_i + 4h), \\ 0, & u \notin [u_i, u_i + 4h). \end{cases} \tag{37}$$

Given an equidistant knot vector, we call $B_i(u)$ a uniform DT B-spline-like basis function, and the related knot vector U is called a uniform knot vector. On the contrary, given a nonequidistant knot vector, we call $B_i(u)$ and U a nonuniform DT B-spline-like basis function and a nonuniform knot vector, respectively. Figure 5 illustrates the DT B-spline-like basis function under different shape parameter values. Before discussing the properties of the DT B-spline-like basis function, we prove the following lemma, which is crucial for the discussion of the curves and surfaces.

Lemma 7. *For all possible $i \in Z^+$, $\alpha_i, \beta_i \in [2, +\infty)$, the coefficients $a_i, b_{i.j}, c_{i,j}, d_i$ have the following properties:*

$$
\begin{aligned}
&a_i + b_{i0} + c_{i0} = 1,\\
&b_{i1} + c_{i1} = 1,\\
&b_{i2} + c_{i2} = 1,\\
&b_{i3} + c_{i3} + d_i = 1,\\
&d_i = c_{i+1,0},\\
&b_{i+2,0} = c_{i+1,3},\\
&b_{i+2,3} = a_{i+3},\\
&\left(\frac{\pi}{2h_i}\right)\beta_i d_i = \left(\frac{\pi}{2h_{i+1}}\right)\alpha_{i+1}\left(c_{i+1,1} - c_{i+1,0}\right),\\
&\left(\frac{\pi}{2h_{i+1}}\right)\beta_{i+1}\left(c_{i+1,3} - c_{i+1,2}\right) = \left(\frac{\pi}{2h_{i+2}}\right)\alpha_{i+2}\left(b_{i+2,1}\right.\\
&\quad\left. - b_{i+2,0}\right),\\
&\left(\frac{\pi}{2h_{i+2}}\right)\beta_{i+2}\left(b_{i+2,3} - b_{i+2,2}\right) = -\left(\frac{\pi}{2h_{i+3}}\right)\alpha_{i+3}a_{i+3},\\
&\left(\frac{\pi}{2h_i}\right)^2 2\left(\beta_i - 1\right)^2 d_i = \left(\frac{\pi}{2h_{i+1}}\right)^2\left\{2\left(\alpha_{i+1} - 1\right)^2 c_{i+1,0}\right.\\
&\quad\left. + \left[-2 - 2\left(\alpha_{i+1} - 1\right)^2\right]c_{i+1,1} + 2c_{i+1,2}\right\},\\
&\left(\frac{\pi}{2h_{i+1}}\right)^2\left\{2c_{i+1,1} + c_{i+1,2}\left[-2 - 2\left(\beta_{i+1} - 1\right)^2\right]\right.\\
&\quad\left. + 2\left(\beta_{i+1} - 1\right)^2 c_{i+1,3}\right\},\\
&= \left(\frac{\pi}{2h_{i+2}}\right)^2\left\{2\left(\alpha_{i+2} - 1\right)^2 b_{i+2,0}\right.\\
&\quad\left. + \left[-2 - 2\left(\alpha_{i+2} - 1\right)^2\right]b_{i+2,1} + 2b_{i+2,2}\right\},\\
&\left(\frac{\pi}{2h_{i+2}}\right)^2\left\{2b_{i+2,1} + b_{i+2,2}\left[-2 - 2\left(\beta_{i+2} - 1\right)^2\right]\right.\\
&\quad\left. + b_{i+2,3}2\left(\beta_{i+2} - 1\right)^2\right\} = \left(\frac{\pi}{2h_{i+3}}\right)^2 2\left(\alpha_{i+3} - 1\right)^2,
\end{aligned}
\tag{38}
$$

Proof. The aforementioned expressions of the coefficients $a_i, b_{i.j}, c_{i,j}, d_i$ show that $d_i = c_{i+1,0}, b_{i+2,0} = c_{i+1,3}$ and $b_{i+2,3} = a_{i+3}$. Straightforward computation yields

$$
\begin{aligned}
b_{i0} &= \frac{\alpha_i\phi_i h_{i-1}}{\mu_{i-1}}a_{i+1} + \frac{\beta_{i-1}\varphi_{i-1}h_i}{\mu_{i-1}}d_{i-2} = \frac{\alpha_i h_{i-1}}{\mu_{i-1}}\\
&\cdot\frac{\lambda_i h_i + \mu_i h_{i+1}}{\beta_i h_{i+1}^2}\frac{\beta_i\lambda_{i-1}h_{i+1}^2}{\lambda_i\mu_{i-1}h_{i-1} + \lambda_{i-1}\lambda_i h_i + \lambda_{i-1}\mu_i h_{i+1}}\\
&+ \frac{\beta_{i-1}h_i}{\mu_{i-1}}\frac{\lambda_{i-2}h_{i-1} + \mu_{i-2}h_{i-2}}{\alpha_{i-1}h_{i-2}^2}\\
&\cdot\frac{\alpha_{i-1}\lambda_{i-1}h_{i-2}^2}{\lambda_{i-1}\mu_{i-2}h_{i-2} + \lambda_{i-2}\lambda_{i-1}h_{i-1} + \lambda_{i-2}\mu_{i-1}h_i}\\
&= \frac{\alpha_i h_{i-1}}{\mu_{i-1}}\left(1 - \frac{\lambda_i\mu_{i-1}h_{i-1}}{\lambda_i\mu_{i-1}h_{i-1} + \lambda_{i-1}\lambda_i h_i + \lambda_{i-1}\mu_i h_{i+1}}\right)\\
&+ \frac{\beta_{i-1}h_i}{\mu_{i-1}}\left(1\right.\\
&\left. - \frac{\lambda_{i-2}\mu_{i-1}h_i}{\lambda_{i-1}\mu_{i-2}h_{i-2} + \lambda_{i-2}\lambda_{i-1}h_{i-1} + \lambda_{i-2}\mu_{i-1}h_i}\right) = 1\\
&- a_i - d_{i-1}.
\end{aligned}
\tag{39}
$$

Similarly, $c_{i,3} = 1 - a_{i+1} - d_i$. Thus, we have $a_i + b_{i0} + c_{i0} = 1$ and $b_{i3} + c_{i3} + d_i = 1$. For $b_{i1} + c_{i1}$ and $b_{i2} + c_{i2}$, we have

$$
\begin{aligned}
b_{i1} + c_{i1} &= \phi_i a_{i+1} + \frac{\mu_{i-1}}{\alpha_i h_{i-1}}d_{i-1} = \frac{\lambda_i h_i + \mu_i h_{i+1}}{\beta_i h_{i+1}^2}\\
&\cdot\frac{\beta_i\lambda_{i-1}h_{i+1}^2}{\lambda_i\mu_{i-1}h_{i-1} + \lambda_{i-1}\lambda_i h_i + \lambda_{i-1}\mu_i h_{i+1}}\\
&+ \frac{\alpha_i h_{i-1} + \beta_{i-1}h_i}{\alpha_i h_{i-1}}\\
&\cdot\frac{\alpha_i\lambda_i h_{i-1}^2}{\lambda_i\mu_{i-1}h_{i-1} + \lambda_{i-1}\lambda_i h_i + \lambda_{i-1}\mu_i h_{i+1}}
\end{aligned}
$$

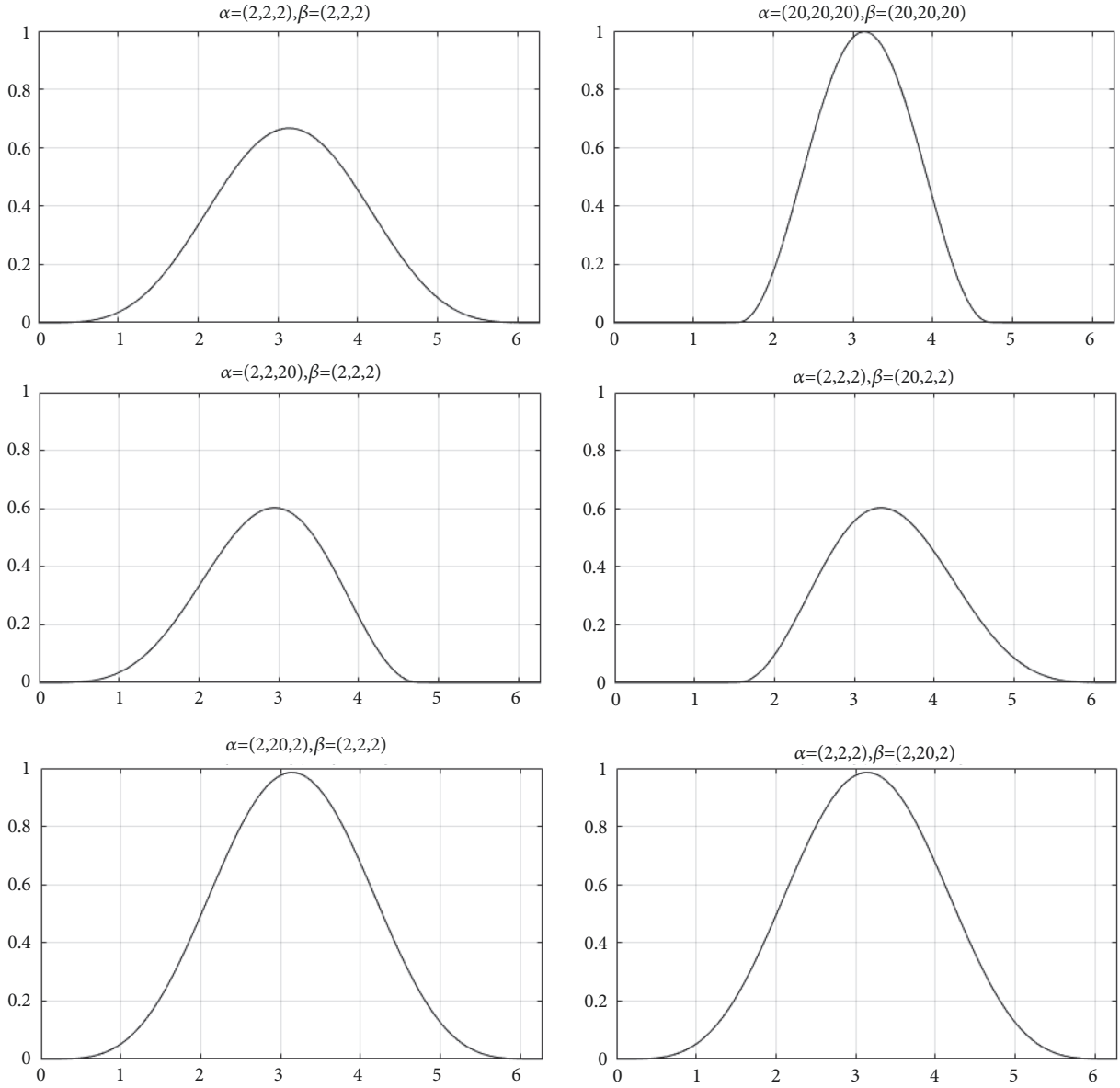

Figure 5: Image of DT B-spline-like basis function.

$$= \frac{\lambda_i\lambda_{i-1}h_i + \mu_i\lambda_{i-1}h_{i+1}}{\lambda_i\mu_{i-1}h_{i-1} + \lambda_{i-1}\lambda_i h_i + \lambda_{i-1}\mu_i h_{i+1}} + \frac{\alpha_i\lambda_i h_{i-1}^2 + \beta_{i-1}\lambda_i h_{i-1}h_i}{\lambda_i\mu_{i-1}h_{i-1} + \lambda_{i-1}\lambda_i h_i + \lambda_{i-1}\mu_i h_{i+1}} = 1, \tag{40}$$

$$b_{i2} + c_{i2} = \frac{\mu_i}{\beta_i h_{i+1}}a_{i+1} + \varphi_i d_{i-1} = \frac{\mu_i}{\beta_i h_{i+1}} \cdot \frac{\beta_i\lambda_{i-1}h_{i+1}^2}{\lambda_i\mu_{i-1}h_{i-1} + \lambda_{i-1}\lambda_i h_i + \lambda_{i-1}\mu_i h_{i+1}} + \frac{\lambda_{i-1}h_i + \mu_{i-1}h_{i-1}}{\alpha_i h_{i-1}^2} \cdot \frac{\alpha_i\lambda_i h_{i-1}^2}{\lambda_i\mu_{i-1}h_{i-1} + \lambda_{i-1}\lambda_i h_i + \lambda_{i-1}\mu_i h_{i+1}}$$

$$= \frac{\mu_i\lambda_{i-1}h_{i+1}}{\lambda_i\mu_{i-1}h_{i-1} + \lambda_{i-1}\lambda_i h_i + \lambda_{i-1}\mu_i h_{i+1}} + \frac{\lambda_i\lambda_{i-1}h_i + \lambda_i\mu_{i-1}h_{i-1}}{\lambda_i\mu_{i-1}h_{i-1} + \lambda_{i-1}\lambda_i h_i + \lambda_{i-1}\mu_i h_{i+1}} = 1. \tag{41}$$

Direct computation provides

$$\left(\frac{\pi}{2h_{i+1}}\right)\alpha_{i+1}\left(c_{i+1,1} - c_{i+1,0}\right) = \left(\frac{\pi}{2h_{i+1}}\right) \cdot \alpha_{i+1}\left(\frac{\mu_i}{\alpha_{i+1}h_i}d_i - d_i\right) = \left(\frac{\pi}{2h_{i+1}}\right)\alpha_{i+1} \cdot \frac{\alpha_{i+1}\lambda_{i+1}h_i^2}{\lambda_{i+1}\mu_i h_i + \lambda_i\lambda_{i+1}h_{i+1} + \lambda_i\mu_{i+1}h_{i+2}}\left(\frac{\mu_i}{\alpha_{i+1}h_i} - 1\right)$$

$$= \left(\frac{\pi}{2h_{i+1}}\right)\alpha_{i+1}$$

$$\cdot \frac{\alpha_{i+1}\lambda_{i+1}h_i^2}{\lambda_{i+1}\mu_i h_i + \lambda_i\lambda_{i+1}h_{i+1} + \lambda_i\mu_{i+1}h_{i+2}}\left(\frac{\beta_i h_{i+1}}{\alpha_{i+1}h_i}\right)$$

$$= \left(\frac{\pi}{2h_i}\right)\beta_i d_i,$$

$$\left(\frac{\pi}{2h_{i+1}}\right)\beta_{i+1}\left(c_{i+1,3} - c_{i+1,2}\right) = \left(\frac{\pi}{2h_{i+1}}\right)$$

$$\cdot \beta_{i+1}\left(\frac{\alpha_{i+2}\phi_{i+2}h_{i+1}}{\mu_{i+1}}a_{i+3} + \frac{\beta_{i+1}\varphi_{i+1}h_{i+2}}{\mu_{i+1}}d_i\right.$$

$$\left. - \varphi_{i+1}d_i\right) = \left(\frac{\pi}{2h_{i+1}}\right)\beta_{i+1}\left(\frac{\alpha_{i+2}\phi_{i+2}h_{i+1}}{\mu_{i+1}}a_{i+3}\right.$$

$$\left. - \frac{\alpha_{i+2}h_{i+1}}{\mu_{i+1}}\varphi_{i+1}d_i\right) = \left(\frac{\pi\alpha_{i+2}\beta_{i+1}}{2\mu_{i+1}}\right)\left(\phi_{i+2}a_{i+3}\right.$$

$$\left. - \varphi_{i+1}d_i\right) = \left(\frac{\pi}{2h_{i+2}}\right)\alpha_{i+2}\left(\phi_{i+2}a_{i+3}\right.$$

$$\left. - \frac{\alpha_{i+2}\phi_{i+2}h_{i+1}}{\mu_{i+1}}a_{i+3} - \frac{\beta_{i+1}\varphi_{i+1}h_{i+2}}{\mu_{i+1}}d_i\right) = \left(\frac{\pi}{2h_{i+2}}\right)$$

$$\cdot \alpha_{i+2}\left(b_{i+2,1} - b_{i+2,0}\right).$$

$$\left(\frac{\pi}{2h_{i+2}}\right)\beta_{i+2}\left(b_{i+2,3} - b_{i+2,2}\right) = \left(\frac{\pi}{2h_{i+2}}\right)\beta_{i+2}\left(a_{i+3}\right.$$

$$\left. - \frac{\mu_{i+2}}{\beta_{i+2}h_{i+3}}a_{i+3}\right) = -\left(\frac{\pi}{2h_{i+3}}\right)\alpha_{i+3}a_{i+3}. \tag{42}$$

Furthermore,

$$\left(\frac{\pi}{2h_{i+1}}\right)^2\left\{2\left(\alpha_{i+1}-1\right)^2 c_{i+1,0}\right.$$

$$\left. + \left[-2 - 2\left(\alpha_{i+1}-1\right)^2\right]c_{i+1,1} + 2c_{i+1,2}\right\} = \left(\frac{\pi}{2h_{i+1}}\right)^2$$

$$\cdot\left\{2\left(\alpha_{i+1}-1\right)^2\left(c_{i+1,0} - c_{i+1,1}\right) + 2\left(c_{i+1,2} - c_{i+1,1}\right)\right\}$$

$$= \left(\frac{\pi}{2h_{i+1}}\right)^2\left\{2\left(\alpha_{i+1}-1\right)^2\left[-\frac{h_{i+1}\beta_i d_i}{h_i\alpha_{i+1}}\right]\right.$$

$$\left. + 2\frac{\lambda_i h_{i+1}}{\alpha_{i+1}h_i^2}d_i\right\} = \left(\frac{\pi}{2h_i}\right)^2 2\left(\beta_i - 1\right)^2 d_i,$$

$$\left(\frac{\pi}{2h_{i+2}}\right)^2\left\{2b_{i+2,1} + b_{i+2,2}\left[-2 - 2\left(\beta_{i+2}-1\right)^2\right]\right.$$

$$\left. + b_{i+2,3}2\left(\beta_{i+2}-1\right)^2\right\} = \left(\frac{\pi}{2h_{i+2}}\right)^2$$

$$\cdot\left\{2\left(b_{i+2,1} - b_{i+2,2}\right) + 2\left(\beta_{i+2}-1\right)^2\left(b_{i+2,3} - b_{i+2,2}\right)\right\}$$

$$= \left(\frac{\pi}{2h_{i+2}}\right)^2\left\{2a_{i+3}\frac{\lambda_{i+2}h_{i+2}}{\beta_{i+2}h_{i+3}^2}\right.$$

$$\left. - 2\left(\beta_{i+2}-1\right)^2\frac{h_{i+2}\alpha_{i+3}}{h_{i+3}\beta_{i+2}}a_{i+3}\right\} = \left(\frac{\pi}{2h_{i+3}}\right)^3 2\left(\alpha_{i+3}\right.$$

$$\left. - 1\right)^2. \tag{43}$$

Finally,

$$\left(\frac{\pi}{2h_{i+1}}\right)^2\left\{2c_{i+1,1} + c_{i+1,2}\left[-2 - 2\left(\beta_{i+1}-1\right)^2\right]\right.$$

$$\left. + 2\left(\beta_{i+1}-1\right)^2 c_{i+1,3}\right\} = \left(\frac{\pi}{2h_{i+1}}\right)^2$$

$$\cdot\left\{2\left(c_{i+1,1} - c_{i+1,2}\right) + 2\left(\beta_{i+1}-1\right)^2\left(c_{i+1,3} - c_{i+1,2}\right)\right\}$$

$$= \left(\frac{\pi}{2h_{i+1}}\right)^2\left\{2\left(c_{i+1,1} - c_{i+1,2}\right)\right.$$

$$\left. + 2\left(\beta_{i+1}-1\right)^2\frac{\alpha_{i+2}h_{i+1}}{h_{i+2}\beta_{i+1}}\left(b_{i+2,1} - b_{i+2,0}\right)\right\}$$

$$= 2\left(\frac{\pi}{2h_{i+1}}\right)^2\left(c_{i+1,1} - c_{i+1,2}\right) + 2\left(\frac{\pi}{2h_{i+1}}\right)^2$$

$$\cdot\left[\frac{\lambda_{i+1}}{h_{i+2}^2\beta_{i+1}} - \frac{\left(\alpha_{i+2}-1\right)^2 h_{i+1}}{h_{i+2}^2}\right]h_{i+1}\left(b_{i+2,1} - b_{i+2,0}\right)$$

$$= 2\left(\frac{\pi}{2h_{i+1}}\right)^2\left(c_{i+1,1} - c_{i+1,2}\right) + 2\left(\frac{\pi}{2h_{i+1}}\right)^2 \tag{44}$$

$$\cdot\frac{\lambda_{i+1}}{h_{i+2}^2\beta_{i+1}}h_{i+1}\left(b_{i+2,1} - b_{i+2,0}\right) + 2\left(\frac{\pi}{2h_{i+2}}\right)^2\left(\alpha_{i+2}\right.$$

$$\left. - 1\right)^2\left(b_{i+2,0} - b_{i+2,1}\right) = -2\left(\frac{\lambda_{i+2}h_{i+2}}{\beta_{i+2}h_{i+3}^2}\right)$$

$$\cdot a_{i+3}\left(\frac{\pi}{2h_{i+2}}\right)^2 + 2\left(\frac{\pi}{2h_{i+2}}\right)^2\left(\alpha_{i+2}-1\right)^2\left(b_{i+2,0}\right.$$

$$\left. - b_{i+2,1}\right) = \left(\frac{\pi}{2h_{i+2}}\right)^2\left\{2\left(\alpha_{i+2}-1\right)^2\left(b_{i+2,0} - b_{i+2,1}\right)\right.$$

$$\left. + 2\left(b_{i+2,2} - b_{i+2,1}\right)\right\} = \left(\frac{\pi}{2h_{i+2}}\right)^2$$

$$\cdot\left\{2\left(\alpha_{i+2}-1\right)^2 b_{i+2,0} + \left[-2 - 2\left(\alpha_{i+2}-1\right)^2\right]b_{i+2,1}\right.$$

$$\left. + 2b_{i+2,2}\right\}.$$

These expressions simplify the lemma. □

3.2. Properties of the DT B-Spline-Like Basis Functions

Theorem 8. *For $u \in [u_3, u_{n+1}]$, we have $\sum_{i=0}^{n} B_i(u) = 1$.*

Proof. For $u \in [u_i, u_{i+1})$, $i = 3, 4, \ldots, n$, $B_j(u) = 0$ for $j \neq i-3, i-2, i-1, i$.

$$\begin{aligned} B_{i-3}(u) &= a_i A_0(t_i; \alpha_i), \\ B_{i-2}(u) &= \sum_{j=0}^{3} b_{i,j} A_j(t_i; \alpha_i, \beta_i), \\ B_{i-1}(u) &= \sum_{j=0}^{3} c_{i,j} A_j(t_i; \alpha_i, \beta_i), \\ B_i(u) &= d_i A_3(t_i, \beta_i), \end{aligned} \tag{45}$$

By using Lemma 7, we have

$$\begin{aligned} \sum_{i=0}^{n} B_i(u) &= a_i A_0(t_i; \alpha_i) + \sum_{j=0}^{3} b_{i,j} A_j(t_i; \alpha_i, \beta_i) \\ &\quad + \sum_{j=0}^{3} c_{i,j} A_j(t_i; \alpha_i, \beta_i) + d_i A_3(t_i; \beta_i) \\ &= \sum_{j=0}^{3} A_j(t_i; \beta_i) = 1. \end{aligned} \tag{46}$$

□

Theorem 9. *If $\alpha_i, \beta_i \in [2, +\infty)$, then $B_i(u) > 0$ for $u_i < u < u_{i+4}$.*

Proof. If $\alpha_i, \beta_i \in [2, +\infty)$, then $a_i, b_{i,j}, c_{i,j}, d_i > 0$ for all possible $i \in Z^+$, $j = 0, 1, 2, 3$. Thus, from the totally positive values of $A_j(t_i; \alpha_i, \beta_i)$, we can immediately induce that $B_i(u) > 0$ for $u_i < u < u_{i+4}$. □

Theorem 10. *For all possible $i \in Z^+$, $\alpha_i, \beta_i \in [2, +\infty)$, the system $\{B_0(u), B_1(u), \ldots, B_n(u)\}$ is linearly independent from $[u_3, u_{n+1}]$.*

Proof. For $\xi_i \in R (i = 0, 1, \ldots, n)$, $u \in [u_3, u_{n+1}]$, let

$$B(u) = \sum_{i=0}^{n} \xi_i B_i(u) = 0. \tag{47}$$

For $\alpha_i, \beta_i \in [2, +\infty)$, direct computation yields

$$\begin{aligned} B(u_i) &= a_i \xi_{i-3} + b_{i,0} \xi_{i-2} + c_{i,0} \xi_{i-1} = 0, \\ B'(u_i) &= \frac{\pi}{2h_i} \left[\alpha_i a_i (\xi_{i-2} - \xi_{i-3}) \right. \\ &\quad \left. + \frac{\beta_{i-1} d_{i-1} h_i}{h_{i-1}} (\xi_{i-1} - \xi_{i-2}) \right] = 0, \\ B''(u_i) &= \left(\frac{\pi}{2h_i} \right)^2 \left[2(\alpha_i - 1)^2 a_i (\xi_{i-3} - \xi_{i-2}) \right. \\ &\quad \left. + \frac{2(\beta_{i-1} - 1)^2 d_{i-1} h_i^2}{h_{i-1}^2} (\xi_{i-1} - \xi_{i-2}) \right] = 0, \end{aligned} \tag{48}$$

where $i = 3, 4, \ldots, n+1$. Thus, we have

$$\begin{aligned} &a_i (\xi_{i-3} - \xi_{i-2}) + (a_i + b_{i,0} + c_{i,0}) \xi_{i-2} \\ &\quad + c_{i,0} (\xi_{i-1} - \xi_{i-2}) = 0, \\ &- \alpha_i a_i (\xi_{i-3} - \xi_{i-2}) + \frac{\beta_{i-1} d_{i-1} h_i}{h_{i-1}} (\xi_{i-1} - \xi_{i-2}) = 0, \\ &(\alpha_i - 1)^2 a_i (\xi_{i-3} - \xi_{i-2}) \\ &\quad + \frac{(\beta_{i-1} - 1)^2 d_{i-1} h_i^2}{h_{i-1}^2} (\xi_{i-1} - \xi_{i-2}) = 0. \end{aligned} \tag{49}$$

Considering that $a_i + b_{i0} + c_{i0} = 1$, we can obtain the following determinant with respect to the aforementioned linear system of equations:

$$\begin{aligned} |M_i| &= \begin{vmatrix} a_i & 1 & c_{i,0} \\ -\alpha_i a_i & 0 & \dfrac{\beta_{i-1} d_{i-1} h_i}{h_{i-1}} \\ (\alpha_i - 1)^2 a_i & 0 & \dfrac{(\beta_{i-1} - 1)^2 d_{i-1} h_i^2}{h_{i-1}^2} \end{vmatrix} \\ &= \frac{a_i d_{i-1} h_i}{h_{i-1}^2} \left[(\beta_{i-1} - 1)^2 h_i \alpha_i + (\alpha_i - 1)^2 \beta_{i-1} h_{i-1} \right] \\ &> 0. \end{aligned} \tag{50}$$

Therefore, $\xi_{i-3} = \xi_{i-2} = \xi_{i-1} = 0$ for $i = 3, 4, \ldots, n+1$. □

Theorem 11. *For $u \in [u_i, u_{i+1}]$, $\alpha_i, \beta_i \in [2, +\infty)$, $i = 3, 4, \ldots, n$, the system $(B_{i-3}(u), B_{i-2}(u), B_{i-1}(u), B_i(u)$ is a totally positive basis of the space span T_{α_i, β_i}.*

Proof. For $u \in [u_i, u_{i+1}]$, $i = 3, 4, \ldots, n$, we can obtain

$$\begin{aligned} &(B_{i-3}(u), B_{i-2}(u), B_{i-1}(u), B_i(u)) \\ &\quad = (A_0(t_i; \alpha_i), A_1(t_i; \alpha_i), A_2(t_i; \beta_i), A_3(t_i; \beta_i)) H_i, \end{aligned} \tag{51}$$

where

$$H_i = \begin{bmatrix} a_i & b_{i,0} & c_{i,0} & 0 \\ 0 & b_{i,1} & c_{i,1} & 0 \\ 0 & b_{i,2} & c_{i,2} & 0 \\ 0 & b_{i,3} & c_{i,3} & d_i \end{bmatrix} \tag{52}$$

and $\alpha_i, \beta_i \in [2, +\infty)$, $t_i(u) = (u - u_i)/h_i$. Given that the system $(A_0(t_i; \alpha_i), A_1(t_i; \alpha_i), A_2(t_i; \beta_i), A_3(t_i; \beta_i))$ is the B-basis of the space T_{α_i, β_i}, according to Theorem 4.2 in [41], we can conclude that H_i is a nonsingular stochastic and totally positive matrix.

For arbitrary $\alpha_i, \beta_i \in [2, +\infty)$, we have $a_i, b_{i,j}, c_{i,j}, d_i > 0$ for all possible $i \in Z^+$, $j = 0, 1, 2, 3$. Moreover, we can conclude that H_i is stochastic from Lemma 7. Straightforward computation provides

$$\begin{aligned}
&\begin{vmatrix} b_{i,0} & c_{i,0} \\ b_{i,1} & c_{i,1} \end{vmatrix} = \frac{\beta_{i-1}\varphi_{i-1}h_i}{\alpha_i h_{i-1}} d_{i-2}d_{i-1} > 0,\\
&\begin{vmatrix} b_{i,0} & c_{i,0} \\ b_{i,2} & c_{i,2} \end{vmatrix}\\
&\quad = \frac{h_i\left(\lambda_{i-1}\mu_i h_{i+1} + \lambda_{i-1}\lambda_i h_i + \lambda_i\mu_{i-1}h_{i-1}\right)}{\beta_i\mu_{i-1}h_{i-1}h_{i+1}^2} a_{i+1}d_{i-1}\\
&\qquad + \frac{\beta_{i-1}\varphi_{i-1}\varphi_i h_i}{\mu_{i-1}} d_{i-2}d_{i-1} > 0,\\
&\begin{vmatrix} b_{i,0} & c_{i,0} \\ b_{i,3} & c_{i,3} \end{vmatrix}\\
&\quad = \frac{\alpha_i\alpha_{i+1}\phi_i\phi_{i+1}h_{i-1}h_i}{\mu_{i-1}\mu_i} a_{i+1}a_{i+2}\\
&\qquad + \frac{h_i\left(\lambda_{i-1}\mu_i h_{i+1} + \lambda_{i-1}\lambda_i h_i + \lambda_i\mu_{i-1}h_{i-1}\right)}{\mu_{i-1}\mu_i h_{i-1}h_{i+1}} a_{i+1}d_{i-1}\\
&\qquad + \frac{\alpha_{i+1}\beta_{i-1}\phi_{i+1}\varphi_{i-1}h_i^2}{\mu_{i-1}\mu_i} a_{i+2}d_{i-2}\\
&\qquad + \frac{\beta_{i-1}\beta_i\varphi_{i-1}\varphi_i h_i h_{i+1}}{\mu_{i-1}\mu_i} d_{i-2}d_{i-1} > 0,\\
&\begin{vmatrix} b_{i,1} & c_{i,1} \\ b_{i,2} & c_{i,2} \end{vmatrix}\\
&\quad = \frac{h_i\left(\lambda_{i-1}\mu_i h_{i+1} + \lambda_{i-1}\lambda_i h_i + \lambda_i\mu_{i-1}h_{i-1}\right)}{\alpha_i\beta_i\mu_{i-1}h_{i-1}^2h_{i+1}^2} a_{i+1}d_{i-1}\\
&\quad > 0,\\
&\begin{vmatrix} b_{i,1} & c_{i,1} \\ b_{i,3} & c_{i,3} \end{vmatrix}\\
&\quad = \frac{h_i\left(\lambda_{i-1}\mu_i h_{i+1} + \lambda_{i-1}\lambda_i h_i + \lambda_i\mu_{i-1}h_{i-1}\right)}{\alpha_i\mu_i h_{i-1}^2 h_{i+1}} a_{i+1}d_{i-1}\\
&\qquad + \frac{\alpha_{i+1}\phi_i\phi_{i+1}h_i}{\mu_i} a_{i+1}a_{i+2} > 0,\\
&\begin{vmatrix} b_{i,2} & c_{i,2} \\ b_{i,3} & c_{i,3} \end{vmatrix} = \frac{\alpha_{i+1}\phi_{i+1}h_i}{\beta_i h_{i+1}} a_{i+1}a_{i+2} > 0.
\end{aligned} \tag{53}$$

This verification shows that H_i is also a totally positive matrix and thus proves the theorem. □

Theorem 12. *For arbitrary $\alpha_i, \beta_i \in [2, +\infty)$, given a nonuniform knot vector, $B_i(u)$ has C^2 continuity at each knot.*

Proof. Without loss of generality, we consider the knot u_{i+1}. For arbitrary $\alpha_i, \beta_i \in [2, +\infty)$, we have

$$\begin{aligned}
&B_i\left(u_{i+1}^-\right) = d_i,\\
&B_i\left(u_{i+1}^+\right) = c_{i+1,0},\\
&B_i'\left(u_{i+1}^-\right) = \frac{\pi}{2}\cdot\frac{\beta_i d_i}{h_i},\\
&B_i'\left(u_{i+1}^+\right) = \frac{\pi}{2}\cdot\frac{\alpha_{i+1}\left(c_{i+1,1} - c_{i+1.0}\right)}{h_{i+1}},\\
&B''\left(u_{i+1}^-\right) = \left(\frac{\pi}{2}\right)^2\frac{2\left(\beta_i - 1\right)^2 d_i}{h_i^2},\\
&B''\left(u_{i+1}^+\right) = \left(\frac{\pi}{2}\right)^2\\
&\quad\cdot\frac{\left[2\left(\alpha_{i+1} - 1\right)^2\left(c_{i+1,0} - c_{i+1,1}\right) + 2\left(c_{i+1,2} - c_{i+1,1}\right)\right]}{h_{i+1}^2}.
\end{aligned} \tag{54}$$

From the aforementioned calculations and Lemma 7, we can easily find that the theorem is established at knot u_{i+1}. The case of the continuity at other knots can be discussed similarly. □

Theorem 13. *For arbitrary $\alpha_i = \beta_i = 2$, given a nonuniform knot vector, $B_i(u)$ has $C^{2n-1}(n = 1, 2, 3, \ldots)$ continuity at each knot.*

Proof. We use mathematical induction to prove that the $(2n-1)$-order derivative of basis function (22) has the following form:

$$\begin{aligned}
A_0^{(2n-1)} &= (-1)^n\left[\left(2\cos t + 2^{2n-2}\sin 2t\right\right],\\
A_1^{(2n-1)} &= (-1)^n 2\left(-\cos t + 2^{2n-2}\sin 2t\right),\\
A_2^{(2n-1)} &= (-1)^n 2\left(\sin t - 2^{2n-2}\sin 2t\right),\\
A_3^{(2n-1)} &= (-1)^n\left[-2\sin t + 2^{2n-2}\sin 2t\right].
\end{aligned} \tag{55}$$

When $n = 1$, the derivative of the basis functions (22) is

$$\begin{aligned}
A_0' &= -2\cos t - \sin 2t,\\
A_1' &= 2\left(\cos t - \sin 2t\right),\\
A_2' &= 2\left(-\sin t + \sin 2t\right),\\
A_3' &= 2\sin t - \sin 2t.
\end{aligned} \tag{56}$$

These forms are satisfied when $n = 1$.

We assume that the aforementioned forms are also satisfied when $n = k$. Therefore, the $(2k-1)$-order derivative of the basis functions (22) is

$$
\begin{aligned}
A_0^{(2k-1)} &= (-1)^k \left[(2\cos t + 2^{2k-2}\sin 2t\right], \\
A_1^{(2k-1)} &= (-1)^k 2\left(-\cos t + 2^{2k-2}\sin 2t\right), \\
A_2^{(2k-1)} &= (-1)^k 2\left(\sin t - 2^{2k-2}\sin 2t\right), \\
A_3^{(2k-1)} &= (-1)^k \left[-2\sin t + 2^{2k-2}\sin 2t\right].
\end{aligned} \tag{57}
$$

By direct computing, we have

$$
\begin{aligned}
\left[A_0^{(2k-1)}\right]'' &= (-1)^{k+1}\left[(2\cos t + 2^{2(k+1)-2}\sin 2t\right], \\
\left[A_1^{(2k-1)}\right]'' &= (-1)^{k+1} 2\left(-\cos t + 2^{2(k+1)-2}\sin 2t\right), \\
\left[A_2^{(2k-1)}\right]'' &= (-1)^{k+1} 2\left(\sin t - 2^{2(k+1)-2}\sin 2t\right), \\
\left[A_3^{(2k-1)}\right]'' &= (-1)^{k+1}\left[-2\sin t + 2^{2(k+1)-2}\sin 2t\right].
\end{aligned} \tag{58}
$$

These forms are satisfied when $n = k + 1$. In summary, the $2n - 1$-order derivative of the basis functions (22) has the form of (55). Finally, we prove that the basis function $B_i(u)$ is C^{2n-1} $(n = 1, 2, \ldots)$ continuous at each knot.

Without loss of generality, we first consider the continuity at the knot u_{i+1}. From here and Remark 6, direct computation gives

$$
\begin{aligned}
B_i^{(2n-1)}\left(u_{i+1}^-\right) &= (-1)^2 \cdot (-2) \cdot \frac{1}{6}, \\
B_i^{(2n-1)}\left(u_{i+1}^+\right) &= (-1)^2 \cdot 2 \cdot \frac{1}{6} + (-1)^2 \cdot 2 \cdot \frac{1}{3} \cdot (-1) \\
&= (-1)^2 \cdot (-2) \cdot \frac{1}{6}.
\end{aligned} \tag{59}
$$

Thus, we can immediately conclude that $B_i^{(2n-1)}(u_{i+1}^+) = B_i^{(2n-1)}(u_{i+1}^-)$ for a uniform knot vector and all $\alpha_i = \beta_i = 2$. In summary, the theorem is established at knot u_{i+1}. The continuity of the basis functions with respect to other knots can be discussed similarly. □

3.3. DT B-Spline-Like Curves

Definition 14. Given control points P_i $(i = 0, 1, \ldots, n)$ in R^2 or $R^3$and a knot vector U, for arbitrary real numbers $\alpha_i, \beta_i \in [2, +\infty), n \geq 3, u \in [u_3, u_{n+1}]$,

$$
B(u) = \sum_{i=0}^{n} B_i(u) P_i \tag{60}
$$

is called a DT B-spline-like curve with two denominator shape parameters α_i, β_i.

For $u \in [u_i, u_{i+1}]$, $i = 3, 4, \ldots, n$, we rewrite (60) as the following curve segment:

$$
\begin{aligned}
B(u) &= \sum_{j=i-3}^{i} B_j(u) P_j \\
&= \left(a_i P_{i-3} + b_{i0} P_{i-2} + c_{i0} P_{i-1}\right) A_0\left(t_i; \alpha_i\right) \\
&\quad + \left(b_{i1} P_{i-2} + c_{i1} P_{i-1}\right) A_1\left(t_i; \alpha_i\right) \\
&\quad + \left(b_{i2} P_{i-2} + c_{i2} P_{i-1}\right) A_2\left(t_i; \beta_i\right) \\
&\quad + \left(b_{i3} P_{i-2} + c_{i3} P_{i-1} + d_i P_i\right) A_3\left(t_i; \beta_i\right).
\end{aligned} \tag{61}
$$

From Theorems 9 and 10, $B(u)$ possesses affine invariance and lies in the convex hull of the points $P_{i-3}, P_{i-2}, P_{i-1}, P_i$ for $u \in [u_i, u_{i+1}]$. Theorem 11 shows that $B(u)$ possesses the variation diminishing property, indicating that $B(u)$ is suitable for curve design. From Theorem 12, we can introduce the following theorem.

Theorem 15. *Given a non-uniform knot vector, $B(u)$ has C^2 continuity at each knot. Furthermore, considering the simple knot u_i $(i = 3, 4, \ldots, n + 1)$, we have*

$$
\begin{aligned}
B\left(u_i\right) &= a_i P_{i-3} + b_{i0} P_{i-2} + c_{i0} P_{i-1}, \\
B'\left(u_i\right) &= \frac{\pi}{2}\left[\frac{1}{h_i}\alpha_i a_i \left(P_{i-2} - P_{i-3}\right)\right. \\
&\quad \left. + \frac{\beta_{i-1} d_{i-1}}{h_{i-1}}\left(P_{i-1} - P_{i-2}\right)\right], \\
B''\left(u_i\right) &= \left(\frac{\pi}{2}\right)^2\left[\frac{2}{h_i^2}\left(\alpha_i - 1\right)^2 a_i \left(P_{i-3} - P_{i-2}\right)\right. \\
&\quad \left. + \frac{2\left(\beta_{i-1} - 1\right)^2 d_{i-1}}{h_{i-1}^2}\left(P_{i-1} - P_{i-2}\right)\right].
\end{aligned} \tag{62}
$$

Theorem 16. *Given a uniform knot vector, $B(u)$ has C^{2n-1} $(n = 1, 2, 3, \ldots)$ continuity for all $a_i = \beta_i = 2$ at each knot.*

Proof. Without loss of generality, we consider the knot u_{i+1}. From Theorem 15 and Remark 6, for all $a_i = \beta_i = 2$, we have

$$
\begin{aligned}
B_i\left(u_{i+1}^-\right) &= \frac{1}{6} A_3\left(t_i\right), \\
B_i\left(u_{i+1}^+\right) &= \frac{1}{6} A_0\left(t_{i+1}\right) + \frac{1}{3} A_1\left(t_{i+1}\right) + \frac{2}{3} A_2\left(t_{i+1}\right) \\
&\quad + \frac{2}{3} A_3\left(t_{i+1}\right), \\
B_i^{(2n-1)}\left(u_{i+1}^+\right) &= \frac{1}{6} A_3^{(2n-1)}\left(t_i\right) \\
&= \frac{1}{6}(-1)^n\left(-2\sin t + 2^{2n-2}\sin 2t\right) \\
&= -\frac{1}{3}(-1)^n, \\
B_i^{(2n-1)}\left(u_{i+1}^-\right) &= \frac{1}{6} A_0^{(2n-1)}\left(t_i\right) + \frac{1}{3} A_1^{(2n-1)}\left(t_i\right) \\
&\quad + \frac{2}{3} A_2^{(2n-1)}\left(t_i\right) + \frac{2}{3} A_3^{(2n-1)}\left(t_i\right) \\
&= \frac{1}{6}(-1)^n\left[(2\cos t + 2^{2n-2}\sin 2t\right]
\end{aligned}
$$

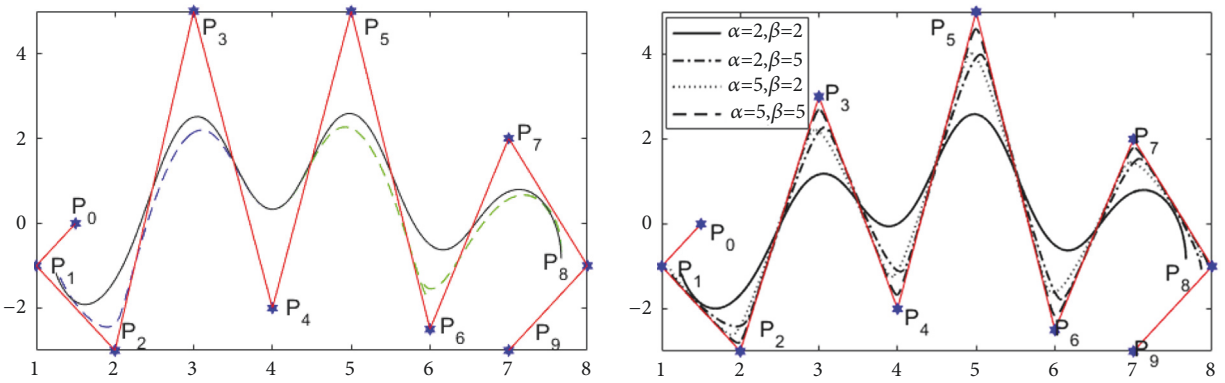

FIGURE 6: DT B-spline-like curves.

$$+\frac{1}{3}(-1)^n 2\left(-\cos t + 2^{2n-2}\sin 2t\right)$$
$$+\frac{2}{3}(-1)^n 2\left(\sin t - 2^{2n-2}\sin 2t\right)$$
$$+\frac{2}{3}(-1)^n\left[-2\sin t + 2^{2n-2}\sin 2t\right]$$
$$= -\frac{1}{3}(-1)^n. \tag{63}$$

We can immediately conclude that $B_i^{(2n-1)}(u_{i+1}^+) = B_i^{(2n-1)}(u_{i+1}^+)$ for a uniform knot vector and all $a_i = \beta_i = 2$. In summary, the theorem is established at knot u_{i+1}. The continuity of $B(u)$ with respect to other knots can be similarly discussed.

The DT B-spline-like curve proposed in this study possesses two denominator shape parameters α_i, β_i. Therefore, when the control points are unchanged, we can easily adjust the proposed curve shape by changing the parameter values. From (61), the shape parameters $\alpha_{i-1}, \alpha_i, \alpha_{i+1}, \alpha_{i+2}, \beta_{i-2}, \beta_{i-1}, \beta_i, \beta_{i+1}$ affect the curve segment $B(u)$, $u \in [u_i, u_{i+1}]$. Therefore, shape parameters α_i affect four curve segments $[u_{i-2}, u_{i+2}]$, and β_i affects four curve segments $[u_{i-1}, u_{i+3}]$. Furthermore, the shape of the proposed curve can be predicted on the basis of the shape parameter value. As α_i and β_i increase, the coefficients of control points P_{i-3} and P_i decrease while the coefficients of P_{i-2} and P_{i-1} increase. Therefore, as α_i and β_i increase simultaneously, the curve segments $B(u)(u \in [u_i, u_{i+1}])$ tend to $P_{i-2}P_{i-1}$. If α_i and β_i increase, the curve segments $B(u)(u \in [u_i, u_{i+1}])$ will tend to control point P_{i-2} or P_{i-1}, respectively.

Figure 6 shows $B(u)$ with different denominator shape parameters. The left figure shows $B(u)$, which is generated by setting all $\alpha_i = \beta_i = 2$ (black lines); the blue line is generated by changing one α_i to 4; and the green line is generated by changing one β_i to 4. The right figure shows that $B(u)$ is generated by setting all $\alpha_i = 2$ *or* 5 and $\beta_i = 2$ *or* 5. □

3.4. DT B-Spline-Like Surface

Definition 17. Given control points P_{ij} $(i = 0, 1, \ldots, m,\ j = 0, 1, \ldots, n)$ in R^3 and two knot vectors $U = (u_0, u_1, \ldots, u_{n+4})$, $V = (v_0, v_1, \ldots, v_{n+4})$, for arbitrary real numbers $\alpha_{ij}, \beta_{ij} \in [2, +\infty), m, n \geq 3, u \in [u_3, u_{m+1}], v \in [v_3, v_{n+3}]$,

$$B(u, v) = \sum_{i=0}^{m}\sum_{j=0}^{n} B_i(u) B_j(v) P_{ij} \tag{64}$$

is called a DT B-spline-like surface with four denominator shape parameters, namely, $\alpha_{i1}, \beta_{i1}, \alpha_{j2}, \beta_{j2}$, where α_{i1}, β_{i1} belong to basis function $B_i(u)$ and α_{j2}, β_{j2} belong to basis function $B_j(u)$.

Theorem 18. *Given two nonuniform knot vectors U and V, the DT B-spline-like surface $B(u, v)$ possesses C^2 continuity at each knot.*

Theorem 19. *For $u \in [u_3, u_{m+1}]$, $v \in [v_3, v_{n+1}]$, the DT B-spline-like surface $B(u, v)$ possesses C^{2n-1} $(n = 1, 2, 3, \ldots)$ continuity for all $a_{ij} = \beta_{ij} = 2$ at each knot.*

Proof. Without loss of generality, we consider the continuity at the region $[u_i, u_{i+1}) \times [v_j, v_{j+1})$. For $u \in [u_i, u_{i+1})$, $v \in [v_j, v_{j+1}), i = 3, 4, \ldots, m$, $j = 3, 4, \ldots, n$, $B_k(u) = 0$, $B_l(v) = 0$ for $k \neq i-3, i-2, i-1, l \neq j-3, j-2, j-1, j$.

$$\begin{aligned}
B_i(u) &= a_i A_0(t_i; \alpha_i),\\
B_{i-1}(u) &= \sum_{k=0}^{3} b_{i,k} A_k(t_i; \alpha_i, \beta_i),\\
B_{i-2}(u) &= \sum_{k=0}^{3} c_{i,k} A_k(t_i; \alpha_i, \beta_i),\\
B_{i-3}(u) &= d_i A_3(t_i, \beta_i),\\
B_j(u) &= a_j A_0(t_j; \alpha_j),\\
B_{j-1}(u) &= \sum_{l=0}^{3} b_{j,l} A_l(t_j; \alpha_j, \beta_j),\\
B_{j-2}(u) &= \sum_{l=0}^{3} c_{j,l} A_l(t_j; \alpha_j, \beta_j),\\
B_{j-3}(u) &= d_j A_3(t_j, \beta_j).
\end{aligned} \tag{65}$$

From Definition 17, we have

$$B_{ij}(u,v)=\sum_{s=i-3}^{i}\sum_{t=j-3}^{j}B_s(u)\,B_t(v)\,P_{st}. \tag{66}$$

We prove that the continuity of the u direction and the continuity of the v direction can be similarly discussed. Considering the continuity at the knot (u_{i+1},v_{i+1}), we have

$$\begin{aligned}&\frac{\delta^{2n-1}B_{ij}\left(u_{i+1}^{-},v_{j+1}\right)}{\delta u^{2n-1}}\\&=\sum_{s=i-3}^{i}\sum_{t=j-3}^{j}\left[\frac{\delta^{2n-1}B_s\left(u_{i+1}^{-}\right)}{\delta u^{2n-1}}\right]B_t\left(v_{j+1}\right)P_{st},\\&\frac{\delta^{2n-1}B_{ij}\left(u_{i+1}^{+},v_{j+1}\right)}{\delta u^{2n-1}}\\&=\sum_{s=i-3}^{i}\sum_{t=j-3}^{j}\left[\frac{\delta^{2n-1}B_s\left(u_{i+1}^{+}\right)}{\delta u^{2n-1}}\right]B_t\left(v_{j+1}\right)P_{st}.\end{aligned} \tag{67}$$

From Theorem 16, for all $a_{ij}=\beta_{ij}=2$, we have

$$\begin{aligned}&\frac{\delta^{2n-1}B_{ij}\left(u_{i+1}^{-},v_{j+1}\right)}{\delta u^{2n-1}}\\&=\sum_{s=i-3}^{i}\sum_{t=j-3}^{j}\left[-\frac{1}{3}(-1)^n\right]B_t\left(v_{j+1}\right)P_{st}\\&=\frac{\delta^{2n-1}B_{ij}\left(u_{i+1}^{+},v_{j+1}\right)}{\delta u^{2n-1}}.\end{aligned} \tag{68}$$

In summary, the theorem is established at knot (u_{i+1},v_{i+1}). The continuity of $B(u,v)$ given in (64) with respect to other knots can be similarly discussed.

The given spline surface $B(u,v)$ possesses four local denominator shape parameters, namely, $\alpha_{i1},\beta_{i1},\alpha_{j2},\beta_{j2}$. By changing the value of the shape parameter, we can adjust the shape of $B(u,v)$ flexibly. According to (66), shape parameters $\alpha_{i1-1},\alpha_{i1},\alpha_{i1+1},\alpha_{i1+2},\ \beta_{i1-2},\beta_{i1-1},\beta_{i1},\beta_{i1+1},\alpha_{i2-1},\alpha_{i2},\alpha_{i2+1},\alpha_{i2+2},\beta_{i2-2},\beta_{i2-1},\ \beta_{i2},\beta_{i2+1}$ affect the surface patch $R(u,v),u\in[u_i,u_{i+1}],v\in[v_j,v_{j+1}]$. Therefore, shape parameters α_{i1},α_{j2} affect surface patch $[u_{i-2},u_{i+2}]\times[v_{j-2},v_{j+2}]$, shape parameters β_{i1},β_{j2} affect surface patch $[u_{i-1},u_{i+3}]\times[v_{j-1},v_{j+3}]$, shape parameters α_{i1},β_{j2} affect the surface patch $[u_{i-2},u_{i+2}]\times[v_{j-1},v_{j+3}]$, and shape parameters α_{j2},β_{i1} affect the surface patch $[u_{i-1},u_{i+3}]\times[v_{j-2},v_{j+2}]$. These results show that parameters $\alpha_{i1},\beta_{i1},\alpha_{j2},\beta_{j2}$ serve to local control tension in the surface. Increasing $\alpha_{i1},\beta_{i1},\alpha_{j2},\beta_{j2}$ locally moves the surface $R(u,v),u\in[u_i,u_{i+1}],\ v\in[v_j,v_{j+1}]$ toward the control polygon. Figure 7 shows $B(u,v)$ with different shape parameters. The figure on the left shows $B(u,v)$ generated when all shape parameters are set $\alpha_{i1}=\beta_{i1}=\alpha_{j2}=\beta_{j2}=2$. The figure on the right shows $B(u,v)$ generated when all shape parameters are set $\alpha_{i1}=\beta_{i1}=\alpha_{j2}=\beta_{j2}=5$. □

4. DT BB-Like Basis with Three Denominator Shape Parameters

4.1. DT BB-Like Basis

Definition 20. For $\alpha,\beta,\gamma\in[2,+\infty)$, $D=\{(u,v,w)\mid u+v+w=\pi/2,u\geq 0,v\geq 0,w\geq 0\}$, the 10 functions given below are considered new cubic DT BB-like basis functions with three denominator shape parameters α, β, and γ over the triangular domain D.

$$\begin{aligned}T_{3,0,0}^{3}(u,v,w;\alpha,\beta,\gamma)&=\frac{(1-\cos u)^2}{1+(\alpha-2)\cos u},\\T_{0,3,0}^{3}(u,v,w;\alpha,\beta,\gamma)&=\frac{(1-\cos v)^2}{1+(\beta-2)\cos v},\\T_{0,0,3}^{3}(u,v,w;\alpha,\beta,\gamma)&=\frac{(1-\cos w)^2}{1+(\gamma-2)\cos w},\\T_{2,1,0}^{3}(u,v,w;\alpha,\beta,\gamma)&=\cos w\sin v(1-\cos u)\frac{\alpha+(\alpha-2)\cos u}{1+(\alpha-2)\cos u}\\T_{2,0,1}^{3}(u,v,w;\alpha,\beta,\gamma)&=\cos v\sin w(1-\cos u)\frac{\alpha+(\alpha-2)\cos u}{1+(\alpha-2)\cos u}\\T_{1,2,0}^{3}(u,v,w;\alpha,\beta,\gamma)&=\cos w\sin u(1-\cos v)\frac{\beta+(\beta-2)\cos v}{1+(\beta-2)\cos v}\\T_{0,2,1}^{3}(u,v,w;\alpha,\beta,\gamma)&=\cos u\sin w(1-\cos v)\frac{\beta+(\beta-2)\cos v}{1+(\beta-2)\cos v}\\T_{1,0,2}^{3}(u,v,w;\alpha,\beta,\gamma)&=\cos v\sin u(1-\cos w)\frac{\gamma+(\gamma-2)\cos w}{1+(\gamma-2)\cos w}\\T_{0,1,2}^{3}(u,v,w;\alpha,\beta,\gamma)&=\cos u\sin v(1-\cos w)\frac{\gamma+(\gamma-2)\cos w}{1+(\gamma-2)\cos w}\\T_{1,1,1}^{3}(u,v,w;\alpha,\beta,\gamma)&=1-\sum_{\substack{i+j+k=3,\\ i\cdot j\cdot k=1}}T_{i,j,k}^{3}(u,v,w;\alpha,\beta,\gamma).\end{aligned} \tag{69}$$

When $w=0$, the 10 DT BB-like basis functions $T_{i,j,k}^{3}(u,v,w;\alpha,\beta,\gamma)$ degenerate to the DT B-like basis functions $A_i(t;\alpha,\beta)$ (notice $v=\pi/2-u$) given in (22). Thus, the DT BB-like basis $T_{i,j,k}^{3}(u,v,w;\alpha,\beta,\gamma)$ is the extension of $A_i(t;\alpha,\beta)$ over the triangular domain.

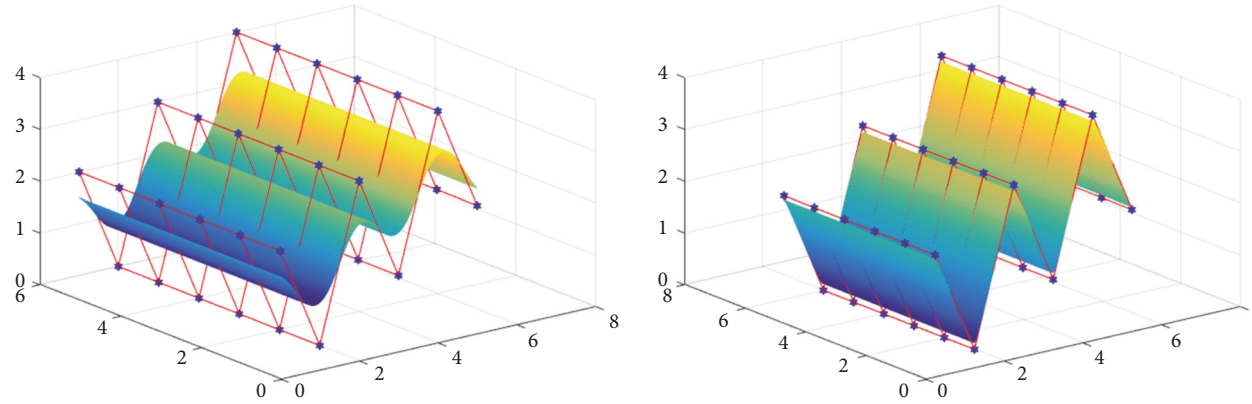

Figure 7: DT B-spline-like surface.

4.2. Properties of the DT BB-Like Basis. In this subsection, we will give important properties of DT BB-like basis functions given in (69).

Theorem 21. *The basis functions given in (69) have the following properties.*

(a) Nonnegativity: $T^3_{i,j,k}(u,v,w;\alpha,\beta,\gamma) \geq 0$, $i,j,k \in N$, $i+j+k=3$.

(b) Partition of unity: $\sum_{i+j+k=3} T^3_{i,j,k}(u,v,w;\alpha,\beta,\gamma) = 1$.

(c) Symmetry: for all $i,j,k \in N, i+j+k=3$, *we have*

$$\begin{aligned} T^3_{i,j,k}(u,v,w;\alpha,\beta,\gamma) &= T^3_{j,i,k}(v,u,w;\beta,\alpha,\gamma) \\ &= T^3_{j,k,i}(v,w,u;\beta,\gamma,\alpha) \\ &= T^3_{i,k,j}(u,w,v;\alpha,\gamma,\beta) \\ &= T^3_{k,i,j}(w,u,v;\gamma,\alpha,\beta) \\ &= T^3_{k,j,i}(w,v,u;\gamma,\beta,\alpha) \end{aligned} \tag{70}$$

(d) Linear independence: $\{T^3_{i,j,k}(u,v,w;\alpha,\beta,\gamma),\ i+j+k=3\}$ *are linearly independent.*

Proof. We include the proofs of (a) and (d) only. The remaining cases can be directly computed.

(a) For any $\alpha,\beta,\gamma \in [2,+\infty)$, $i,j,k \in N$, $i+j+k=3$ and $i\cdot j\cdot k \neq 1$, $T^3_{i,j,k}(u,v,w;\alpha,\beta,\gamma) \geq 0$ is apparent. Furthermore, for $T^3_{1,1,1}(u,v,w;\alpha,\beta,\gamma)$, by directly computing, we have

$$\begin{aligned} &T^3_{1,1,1}(u,v,w;\alpha,\beta,\gamma) \\ &\quad = 1 - \sum_{\substack{i+j+k=3,\\ i\cdot j\cdot k\neq 1}} T^3_{i,j,k}(u,v,w;\alpha,\beta,\gamma) \\ &\quad = 1 - \left(\sin^2 u + \sin^2 v + \sin^2 w\right) \\ &\quad = \frac{1}{2}(\cos 2u + \cos 2v + \cos 2w - 1) \\ &\quad = 2\sin u \sin v \sin w \geq 0. \end{aligned} \tag{71}$$

(d) For $\alpha,\beta,\gamma \in [2,+\infty)$, $\xi_{i,j,k} \in R$ $(i+j+k=3)$, we consider a linear combination

$$\sum_{i+j+k=3} \xi_{i,j,k} T^3_{i,j,k}(u,v,w;\alpha,\beta,\gamma) = 0. \tag{72}$$

For $w=0$, we can immediately induce that $\xi_{i,3-i,0}, i=0,1,2,3$ because the DT B-like basis given in (22) possesses the property of linear independence. In the same way, for $s=t=0$, we have $\xi_{i,0,3-i} = \xi_{0,i,3-i} = 0$, $i=0,1,2,3$. Finally, we have $\xi_{1,1,1}=0$.

These findings imply the theorem.

Figure 8 shows four images of DT BB-like basis functions with the parameter values $\alpha=\beta=\gamma=3$. □

4.3. DT BB-Like Patch

Definition 22. Let $\alpha,\beta,\gamma \in [2,+\infty)$, given control points $Q_{ij} \in R^3 (i,j,k \in N,\ i+j+k=3)$ and a domain triangle $D=\{(u,v,w) \mid u+v+w=\pi/2, u\geq 0, v\geq 0, w\geq 0\}$. We call

$$R(u,v,w) = \sum_{i+j+k=3} T^3_{i,j,k}(u,v,w;\alpha,\beta,\gamma) P_{i,j,k}, \quad (u,v,w) \in D \tag{73}$$

the DT BB-like patch over the triangular domain with three shape denominator parameters α,β,γ.

Next, we provide the properties of the DT BB-like patch given in (73).

(a) Affine invariance and convex hull property: the related patch (73) has affine invariance and convex hull property because the basis functions (69) possess the properties of partition of unity and nonnegativity.

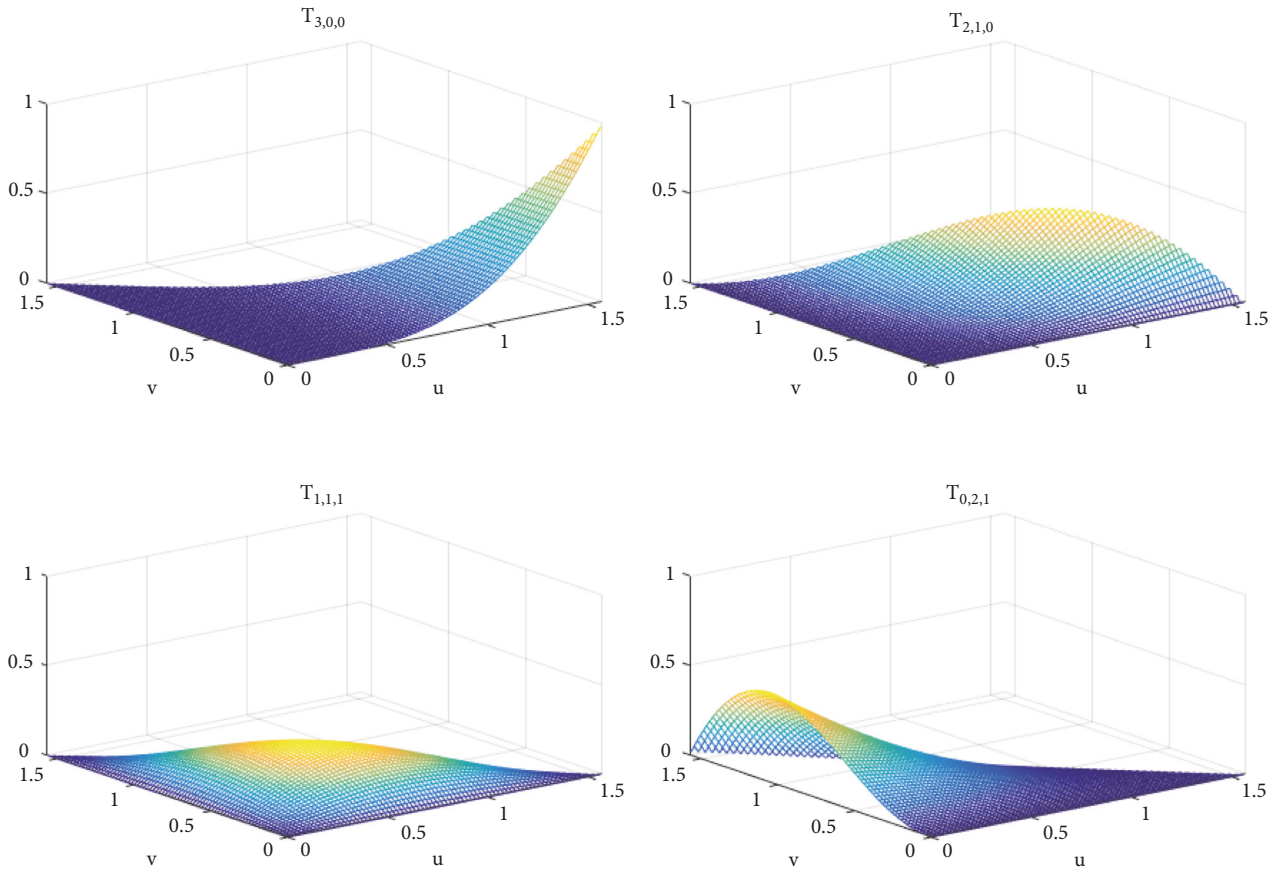

Figure 8: Plots of DT BB-like basis functions.

(b) Geometric property at the corner points: straightforward computation gives

$$R\left(\frac{\pi}{2},0,0\right)=P_{3,0,0},$$
$$R\left(0,\frac{\pi}{2},0\right)=P_{0,3,0},\tag{74}$$
$$R\left(0,0,\frac{\pi}{2}\right)=P_{0,0,3}.$$

(c) Corner point tangent plane: let $w=\pi/2-u-v$. We have

$$\left.\frac{\delta R(u,v,w)}{\delta u}\right|_{(\pi/2,0,0)}=\alpha\left(P_{3,0,0}-P_{2,0,1}\right),$$
$$\left.\frac{\delta R(u,v,w)}{\delta u}\right|_{(\pi/2,0,0)}=\alpha\left(P_{2,1,0}-P_{2,0,1}\right),$$
$$\left.\frac{\delta R(u,v,w)}{\delta u}\right|_{(0,\pi/2,0)}=\beta\left(P_{1,2,0}-P_{0,2,1}\right),$$
$$\left.\frac{\delta R(u,v,w)}{\delta v}\right|_{(0,\pi/2,0)}=\beta\left(P_{0,3,0}-P_{0,2,1}\right),$$
$$\left.\frac{\delta R(u,v,w)}{\delta u}\right|_{(0,0,\pi/2)}=\gamma\left(P_{1,0,2}-P_{0,0,3}\right),$$
$$\left.\frac{\delta R(u,v,w)}{\delta w}\right|_{(0,0,\pi/2)}=\gamma\left(P_{0,1,2}-P_{0,0,3}\right).\tag{75}$$

(d) Boundary property: For $w=0$, $R(u,v,w)$ is a DTB-like curve given in (26), which can be rewritten as

$$R(u,v,0)=\sum_{i=0}^{3}P_{i,3-i,0}A_i(t;\beta,\alpha).\tag{76}$$

This discussion suggests that $R(u,v,w)$ possesses two shape parameters, namely, α and β, when $w=0$. In the same way, when $u=0$ and $v=0$, $R(0,v,w)$ and $R(u,0,w)$ possess shape parameters β,γ and α,γ, respectively. The DTB-like curve can represent elliptic and parabolic arcs when the shape parameters assume a special value (Section 2). Thus, for $\alpha=\beta=\gamma=2$, the three boundaries of the DT BB-like patch can be arcs of an ellipse, circle, and parabola, respectively. Figure 9 shows DT BB-like patches generated by setting $\alpha=\beta=\gamma=2$. The patch whose boundaries are elliptic, circular, and parabolic arcs is shown on the left figure. Its control points are $\{P_{3,0,0}=(0,-4,0),P_{0,3,0}=(2,0,0),P_{0,0,3}=(0,0,2),P_{2,1,0}=(1,-4,0),P_{2,0,1}=(0,-4,1),P_{1,2,0}=(2,0,0),P_{0,2,1}=(2,0,1),P_{1,0,2}=(1,0,2),P_{0,1,2}=(0,-2,2)$, and $P_{1,1,1}=(1,-2,1)\}$.The related boundary parametric equations are $u=0,v=-4\sin x,w=2\cos x;u=2\sin x,v=0,w=2\cos x;$

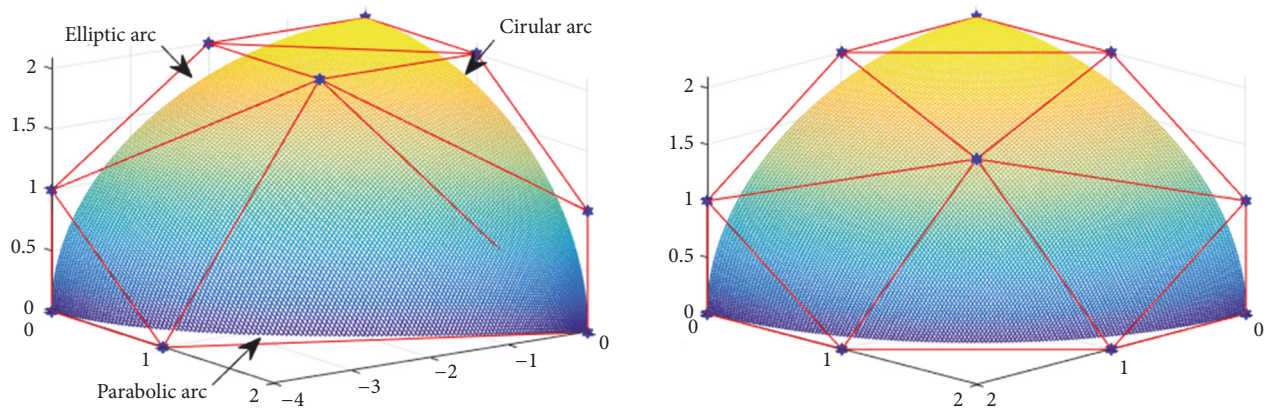

Figure 9: DT BB-like patches whose boundaries are arcs of elliptic, circle, and parabola.

and $u = 2\cos x, v = -4 + 4\cos^2 x, w = 0$ where $x \in [0, \pi/2]$. The right figure shows a patch that possesses three same boundaries as a quarter of the unit circle. The related control points are $\{P_{3,0,0} = (0,2,0), P_{0,3,0} = (2,0,0), P_{0,0,3} = (0,0,2), P_{2,1,0} = (1,2,0), P_{2,0,1} = (0,2,1), P_{1,2,0} = (2,1,0), P_{0,2,1} = (2,0,1), P_{1,0,2} = (0,1,2), P_{0,1,2} = (1,0,2), P_{1,1,1} = (2,-4,2)\}$. The three related parametric equations of the boundaries are $u = 0, v = 2\sin x, w = 2\cos x$; $u = 2\sin x, v = 0, w = 2\cos x$; and $u = 2\cos x, v = 2\sin x, v = 2\sin x, w = 0$, where $x \in [0, \pi/2]$.

(e) Shape adjustable property: by changing the value without changing the control net, we can easily adjust the DT BB-like patch flexibly. As the three denominator shape parameters increase, the patch approaches the control net. Therefore, the three denominator shape parameters are three tension parameters. The three boundaries of the DT BB-like patch are determined by the control points $\{P_{i,j,k}, i+j+k = 3, i \cdot j \cdot k \neq 1\}$, independent of $P_{1,1,1}$. Therefore, the proposed DT BB-like patch (73) can still change the shape by adjusting the control point $P_{1,1,1}$ without changing the three boundaries. In addition, according to the properties of the boundary curve given in (26) of the proposed DT BB-like patch, the three denominator shape parameters α, β, and γ are independent of the boundary curves $R(0, v, w), R(u, 0, w)$, and $R(u, v, 0)$, respectively. This phenomenon also means that when changing the value of a certain denominator parameter, one of the three boundary curves will not be affected. Figure 10 shows the DT BB-like patch under different denominator shape parameters.

4.4. De Casteljau-Type Algorithm. We develop a de Casteljau algorithm that can calculate the DT BB-like patch given in (73). For arbitrary $(u, v, w) \in D$, let

$$
\begin{aligned}
f_1(u,v,w) &:= \frac{\sin u \cos w \left(\sin^2 u + \sin^2 v + \sin^2 w\right)}{\cos w (\sin u + \sin v)\left(\sin^2 u + \sin^2 v + \sin^2 w\right) + \sin w \left(\sin^2 u + \sin^2 v\right)},\\
f_2(u,v,w) &:= \frac{\sin v \cos w \left(\sin^2 u + \sin^2 v + \sin^2 w\right)}{\cos w (\sin u + \sin v)\left(\sin^2 u + \sin^2 v + \sin^2 w\right) + \sin w \left(\sin^2 u + \sin^2 v\right)},\\
f_3(u,v,w) &:= \frac{\sin w \left(\sin^2 u + \sin^2 v\right)}{\cos w (\sin u + \sin v)\left(\sin^2 u + \sin^2 v + \sin^2 w\right) + \sin w \left(\sin^2 u + \sin^2 v\right)},\\
g_1(u,v,w) &:= (1 - \cos u)\left(\sin^2 u + \sin^2 v + \sin^2 w\right),\\
g_2(u,v,w) &:= \sin v \cos w \left(\sin^2 u + \sin^2 v + \sin^2 w\right) + \sin u \sin v \sin w,\\
g_3(u,v,w) &:= \cos v \sin w \left(\sin^2 u + \sin^2 v + \sin^2 w\right) + \sin u \sin v \sin w,
\end{aligned}
\tag{77}
$$

and

$$
\begin{aligned}
P^1_{2,0,0} &:= \frac{1 - \cos u}{(1 + \cos u)[1 + (\alpha - 2)\cos u]} P_{3,0,0}\\
&\quad + \frac{[\alpha - 1 + (\alpha - 2)\cos u]\sin v \cos w}{(1 + \cos u)[1 + (\alpha - 2)\cos u]} P_{2,1,0}\\
&\quad + \frac{[\alpha - 1 + (\alpha - 2)\cos u]\sin w \cos v}{(1 + \cos u)[1 + (\alpha - 2)\cos u]} P_{2,0,1},\\
P^1_{0,2,0} &:= \frac{1 - \cos v}{(1 + \cos v)[1 + (\beta - 2)\cos v]} P_{0,3,0}\\
&\quad + \frac{[\beta - 1 + (\beta - 2)\cos v]\sin u \cos w}{(1 + \cos v)[1 + (\beta - 2)\cos v]} P_{1,2,0}
\end{aligned}
$$

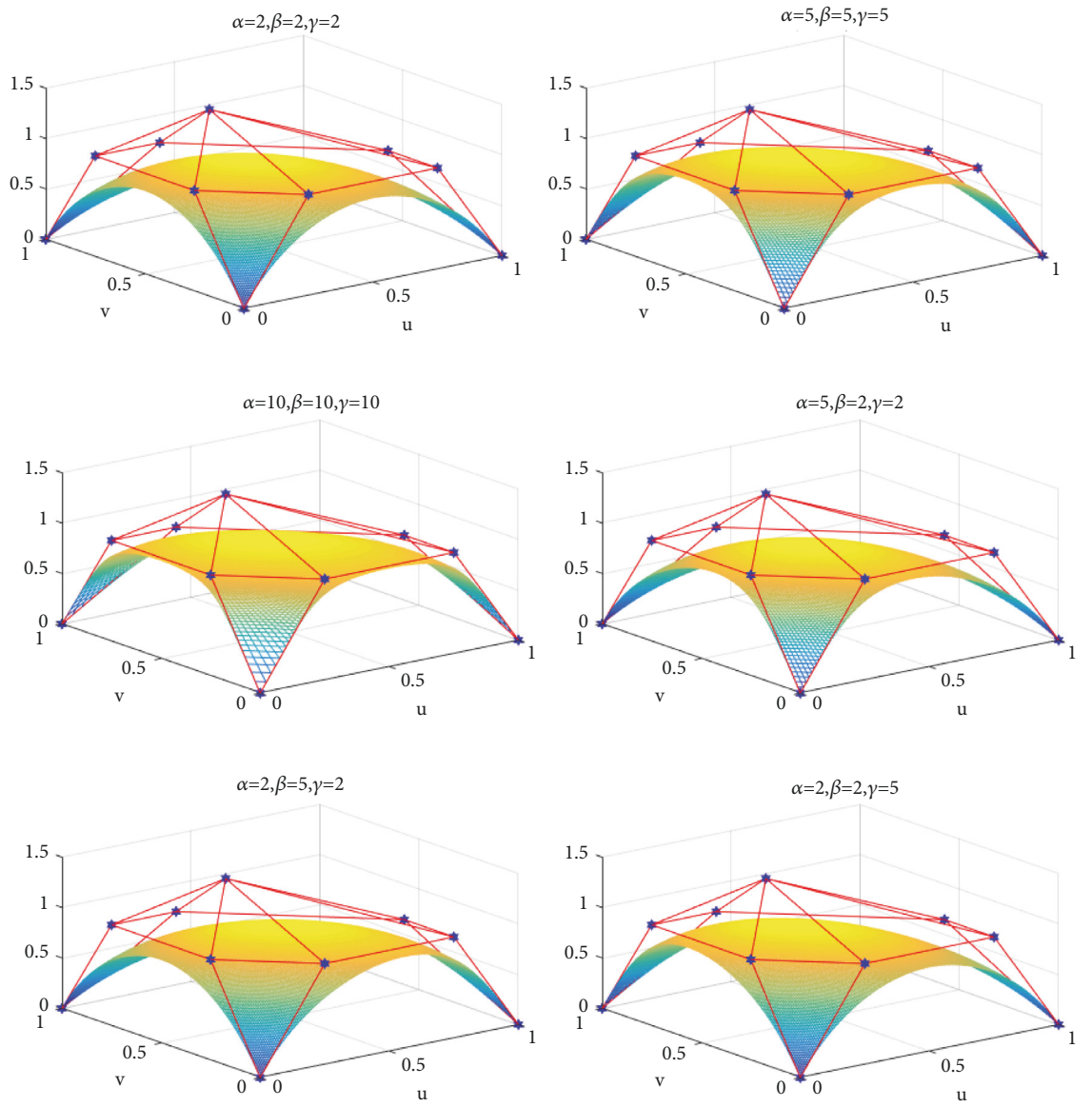

Figure 10: DT BB-like patch with different shape parameters.

$$+\frac{[\beta-1+(\beta-2)\cos v]\sin w\cos u}{(1+\cos v)[1+(\beta-2)\cos v]}P_{0,2,1},$$

$$P^1_{0,0,2}:=\frac{1-\cos u}{(1+\cos u)[1+(\gamma-2)\cos u]}P_{0,0,3}+\frac{[\alpha-1+(\alpha-2)\cos w]\sin u\cos v}{(1+\cos w)[1+(\alpha-2)\cos w]}P_{1,0,2}+\frac{[\gamma-1+(\gamma-2)\cos w]\sin v\cos u}{(1+\cos w)[1+(\gamma-2)\cos w]}P_{0,1,2},$$

$$P^1_{1,1,0}:=f_1(u,v,w)P_{2,1,0}+f_2(u,v,w)P_{1,2,0}+f_3(u,v,w)P_{1,1,1},$$

$$P^1_{1,1,0}:=f_1(u,w,v)P_{2,1,0}+f_2(u,w,v)P_{1,0,2}+f_3(u,w,v)P_{1,1,1},$$

$$P^1_{1,1,0}:=f_1(v,w,u)P_{0,2,1}+f_2(v,w,u)P_{0,1,2}+f_3(v,w,u)P_{1,1,1}. \tag{78}$$

Then we rewrite (73) as

$$R(u,v,w)=\frac{1-\cos^2 u}{\sin^2 u+\sin^2 v+\sin^2 w}\left[g_1(u,v,w)P^1_{2,0,0}+g_2(u,v,w)P^1_{1,1,0}+g_3(u,v,w)P^1_{1,0,1}\right]+\frac{1-\cos^2 v}{\sin^2 u+\sin^2 v+\sin^2 w}\left[g_1(v,u,w)P^1_{0,2,0}\right.$$

$$+ g_2(v,u,w) P^1_{1,1,0} + g_3(v,u,w) P^1_{0,1,1}\Big] + \frac{1-\cos^2 w}{\sin^2 u + \sin^2 v + \sin^2 w}\Big[g_1(w,v,u) P^1_{0,0,2} + g_2(w,v,u) P^1_{0,1,1} + g_3(w,v,u) P^1_{1,0,1}\Big]. \tag{79}$$

Furthermore, by setting

$$\begin{aligned} P^2_{1,0,0} &:= g_1(u,v,w) P^1_{2,0,0} + g_2(u,v,w) P^1_{1,1,0} + g_3(u,v,w) P^1_{1,0,1} \\ P^2_{0,1,0} &:= g_2(v,u,w) P^1_{1,1,0} + g_1(v,u,w) P^1_{0,2,0} + g_3(v,u,w) P^1_{0,1,1} \\ P^2_{0,0,1} &:= g_3(w,v,u) P^1_{1,0,1} + g_2(w,v,u) P^1_{0,1,1} + g_1(w,v,u) P^1_{0,0,2}, \end{aligned} \tag{80}$$

we have

$$\begin{aligned} R(u,v,w) = {} & \frac{1-\cos^2 u}{\sin^2 u + \sin^2 v + \sin^2 w} P^2_{1,0,0} \\ & + \frac{1-\cos^2 v}{\sin^2 u + \sin^2 v + \sin^2 w} P^2_{0,1,0} \\ & + \frac{1-\cos^2 w}{\sin^2 u + \sin^2 v + \sin^2 w} P^2_{0,0,1} := P^3_{0,0,0}. \end{aligned} \tag{81}$$

For $u+v+w = \pi/2$, checking that $f_1(u,v,w)+f_2(u,v,w)+f_3(u,v,w) = 1$ and $g_1(u,v,w) + g_2(u,v,w) + g_3(u,v,w) = 1$ (by using $\sin^2 u+\sin^2 v+\sin^2 w+2\sin u \sin v \sin w = 1$) is easy. Thus (79) and (81) describe the de Casteljau-type algorithm for calculating the DT BB-like patch given in (73).

4.5. Composite Triangular DT BB-Like Patches. Let two DT BB-like patches be

$$R_1(u,v,w) = \sum_{i+j+k=3} T^3_{i,j,k}(u,v,w;\alpha_1,\beta,\gamma) P_{i,j,k}, \quad (u,v,w) \in D, \tag{82}$$

$$R_2(u,v,w) = \sum_{i+j+k=3} T^3_{i,j,k}(u,v,w;\alpha_2,\beta,\gamma) Q_{i,j,k}, \quad (u,v,w) \in D. \tag{83}$$

If the control points satisfy

$$P_{0,j,k} = Q_{0,j,k}, \quad j,k \in N,\ j+k=3, \tag{84}$$

then (82) and (83) possess the common boundary curve $R_1(0,v,w) = R_2(0,v,w), v+w = \pi/2$. Therefore, the two patches form a surface with C^0 continuity.

Differentiating $R_1(0,v,\pi/2-v)$ with respect to v yields

$$\begin{aligned} \frac{dR_1(0,v,\pi/2-v)}{dv} = {} & \frac{\cos v(1-\sin v)\left[\beta+(\beta-2)\sin v\right]}{\left[1+(\beta-2)\sin v\right]^2}\left(P_{0,3,0} - P_{0,2,1}\right) + 2\sin v\cos v\left(P_{0,2,1}-P_{0,1,2}\right) \\ & + \frac{\sin v(1-\cos v)\left[\gamma+(\gamma-2)\cos v\right]}{\left[1+(\gamma-2)\cos v\right]^2}\left(P_{0,1,2} - P_{0,0,3}\right). \end{aligned} \tag{85}$$

For $R_1(u,v,\pi/2-u-v)$ and $R_2(u,v,\pi/2-u-v)$, we differentiate about u. Thus, we have

$$\begin{aligned} \left.\frac{\delta R_1(u,v,\pi/2-v)}{\delta u}\right|_{u=0} = {} & \frac{\cos v(1-\sin v)\left[\beta+(\beta-2)\sin v\right]}{\left[1+(\beta-2)\sin v\right]^2}\left(P_{1,2,0} - P_{0,2,1}\right) + 2\sin v\cos v\left(P_{1,1,1}-P_{0,1,2}\right) \\ & + \frac{\sin v(1-\cos v)\left[\gamma+(\gamma-2)\cos v\right]}{\left[1+(\gamma-2)\cos v\right]^2}\left(P_{1,0,2} - P_{0,0,3}\right), \\ \left.\frac{\delta R_2(u,v,\pi/2-v)}{\delta u}\right|_{u=0} = {} & \frac{\cos v(1-\sin v)\left[\beta+(\beta-2)\sin v\right]}{\left[1+(\beta-2)\sin v\right]^2}\left(Q_{1,2,0} - Q_{0,2,1}\right) + 2\sin v\cos v\left(Q_{1,1,1}-Q_{0,1,2}\right) \\ & + \frac{\sin v(1-\cos v)\left[\gamma+(\gamma-2)\cos v\right]}{\left[1+(\gamma-2)\cos v\right]^2}\left(Q_{1,0,2} - Q_{0,0,3}\right). \end{aligned} \tag{86, 87}$$

For the arbitrary value of v, refer to [44]. If the vectors defined by (85) to (87) are coplanar, then the conditions for G^1 continuous smooth jointing can be achieved. Thus, it can be expressed as

$$\left.\frac{\delta R_2(u,v,\pi/2-u-v)}{\delta u}\right|_{u=0} = \phi\frac{dR_1(0,v,\pi/2-v)}{dv} + \varphi\left.\frac{\delta R_1(u,v,\pi/2-u-v)}{\delta u}\right|_{u=0}, \tag{88}$$

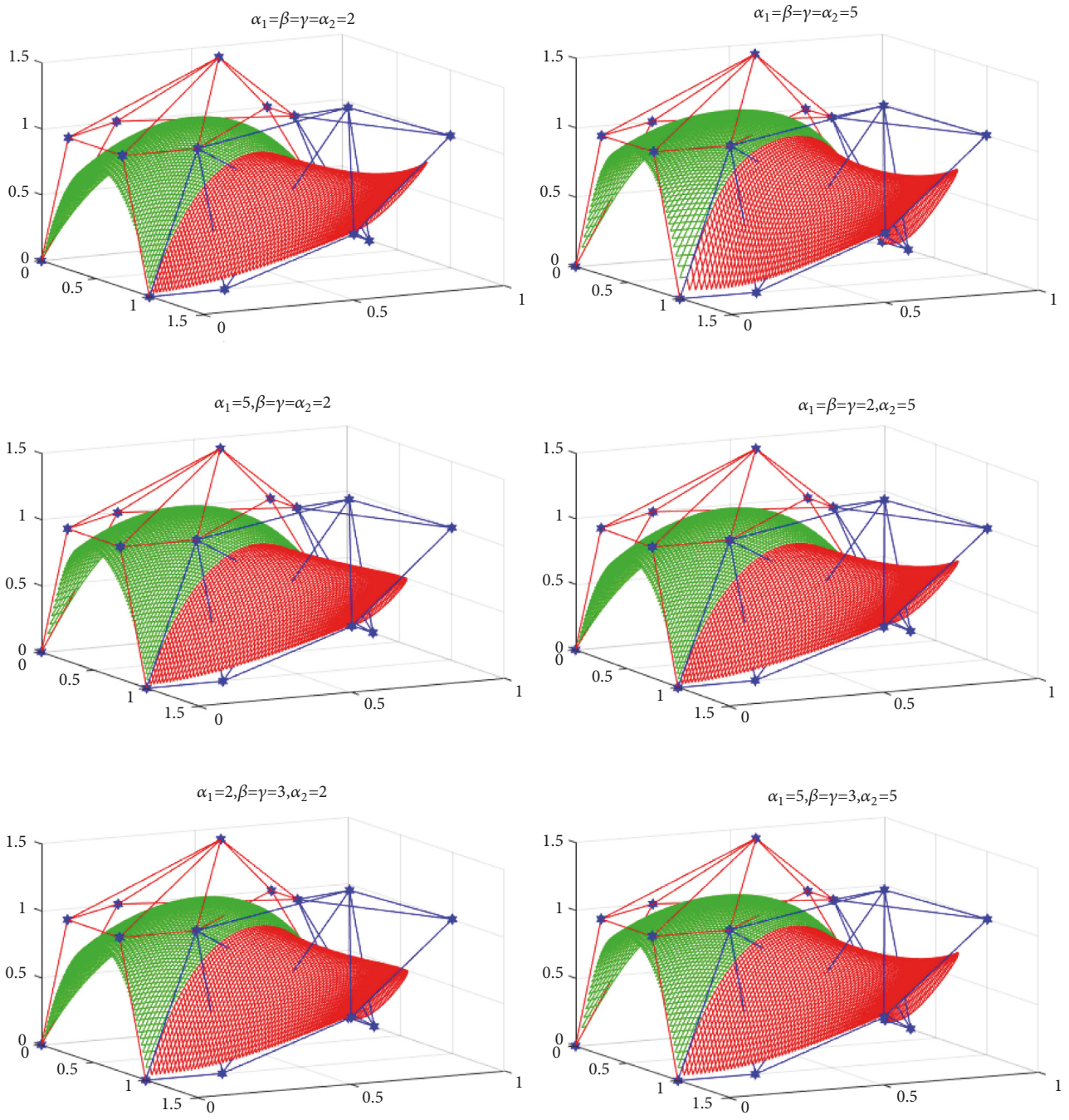

FIGURE 11: G^1 continuous surfaces under different shape parameters.

where ϕ and φ are constants. In summary, we can obtain the following rules:

$$\begin{aligned} Q_{1,2,0} - Q_{0,2,1} &= \phi\left(P_{0,3,0} - P_{0,2,1}\right) + \varphi\left(P_{1,2,0} - P_{0,2,1}\right), \\ Q_{1,1,1} - Q_{0,1,2} &= \phi\left(P_{0,2,1} - P_{0,1,2}\right) + \varphi\left(P_{1,1,1} - P_{0,1,2}\right), \\ Q_{1,0,2} - Q_{0,0,3} &= \phi\left(P_{0,1,2} - P_{0,0,3}\right) + \varphi\left(P_{1,0,2} - P_{0,0,3}\right). \end{aligned} \quad (89)$$

Thus, we can summarize the following theorems.

Theorem 23. *For α_k, β, γ $(k = 1, 2)$, if conditions (84) and (89) hold, then the surface connecting (82) with (83) is G^1 continuous.*

The aforementioned theorem shows that the two DT BB-like patches that connect the conditions are similar to those of the two triangular Bernstein–Bézier-like patches. Detailed content is available in [44]. The only difference is that we can obtain different G^1 continuous surfaces by changing the value of the denominator shape parameter. Figure 11 shows the

G^1 continuous surface under different shape parameters, where $\phi = 1, \varphi = -1$.

5. Conclusion

In this study, the proposed DT B-like basis function forms a set of optimal normalized totally positive bases under the framework of the ECC-space, which leads to the DT BB-spline basis function and the DT-BB-like basis function. Curve and surface construction and related discussions are based on these kinds of basis functions. Compared with the traditional Bézier method and the B-spline technique, the proposed method not only retains all the remarkable properties of the traditional method, such as variation diminishing, but can also accurately represent special industrial curves, such as parabolic and elliptical arcs. In special cases, the B-spline curves and surfaces constructed in this study can automatically reach $C^{(2n-1)}$ $(n = 1, 2, 3, \ldots)$ continuity, thereby satisfying the geometric design requirements of high-order continuity, which is not possible in the traditional literature. In addition, this study introduces a new method for the construction of triangular domain patches. This technique can flexibly adjust the patch with parameters and can accurately represent the boundary as a parabolic arc, an elliptical arc, or even an arc surface. Meanwhile, a de Casteljau algorithm is given to efficiently generate triangular domain patches and the G^1 connecting conditions of the patch. Although the method in this study solves the problem of the traditional method and has many advantages, the construction of the basis function is only the first step. In the design of a curve or surface that is closely in-line with the requirements of the geometric industry, then many problems still need to be addressed. These issues include the accurate quantitative analysis of the influence of the denominator parameter on the DT B-like curve and the DT BB-spline curve; shape analysis of the DT B-like curve and the DT BB-spline curve (convexity, cusp, inflection point, monotonicity, heavy node, etc.); and the higher-order continuous problem analysis of the DT BB-like patch on the triangular domain, except for the G^1 continuity. These issues will be the focus of future research.

Data Availability

The data used to support the findings of this study are available from the corresponding author upon request.

Conflicts of Interest

The authors declare that they have no conflicts of interest.

Acknowledgments

This research was supported by National Natural Science Foundation of China (61861040), the Gansu Education Department Science and Technology Achievement Transformation project (Project no. 2017D-09) and Gansu Province Science and Technology project funding (no. 17YF1FA119).

References

[1] G. Farin, *Curves and surfaces for CAGD*, Morgan Kaufmann, San Francisco, CA, USA, 5th edition, 2001.

[2] J. Hoschek and D. Lasser, *Fundamentals of Computer Aided Geometric Design*, A K Peters, Wellesley, Mass, USA, 1993.

[3] L. Piegl and W. Tiller, *The NURBS Book*, Springer, New York, NY, USA, 1995.

[4] W. Gao and Z. Wu, "A quasi-interpolation scheme for periodic data based on multiquadric trigonometric B-splines," *Journal of Computational and Applied Mathematics*, vol. 271, pp. 20–30, 2014.

[5] C. Manni, F. Pelosi, and M. L. Sampoli, "Generalized B-splines as a tool in isogeometric analysis," *Computer Methods Applied Mechanics and Engineering*, vol. 200, no. 5-8, pp. 867–881, 2011.

[6] Z. Wu, "Piecewise function generated by the solutions of linear ordinary differential equation," in *Third International Congress of CHInese Mathematicians. Part 1, 2*, vol. 2 of *AMS/IP Stud. Adv. Math., 42, pt. 1*, pp. 769–784, Amer. Math. Soc., Providence, RI, 2008.

[7] L. L. Yan and J. F. Liang, "An extension of the Bézier model," *Applied Mathematics and Computation*, vol. 218, no. 6, pp. 2863–2879, 2011.

[8] X. Han, "Cubic trigonometric polynomial curves with a shape parameter," *Computer Aided Geometric Design*, vol. 21, no. 6, pp. 535–548, 2004.

[9] X. Han, "Quadratic trigonometric polynomial curves concerning local control," *Applied Numerical Mathematics*, vol. 56, no. 1, pp. 105–115, 2006.

[10] X. A. Han, Y. C. Ma, and X. L. Huang, "The cubic trigonometric Bézier curve with two shape parameters," *Applied Mathematics Letters*, vol. 22, no. 2, pp. 226–231, 2009.

[11] J. Zhang, "C-curves: an extension of cubic curves," *Computer Aided Geometric Design*, vol. 13, no. 3, pp. 199–217, 1996.

[12] G. M. Nielson, "A locally controllable spline with tension for interactive curve design," *Computer Aided Geometric Design*, vol. 1, no. 3, pp. 199–205, 1984.

[13] B. A. Barsky, "Local control of basis and tension in Beta-splines," *ACM Transactions on Graphics*, pp. 109–134, 1983.

[14] B. A. Barsky, *Computer Graphics and Geometric Modeling Using Beta-Spline*, Computer Science Workbench, Springer-Verlag, Berlin, Heidelberg, Germany, 1988.

[15] J. A. Gregory and M. Sarfraz, "A rational cubic spline with tension," *Computer Aided Geometric Design*, vol. 7, no. 1–4, pp. 1–13, 1990.

[16] P. Costantini and C. Manni, "Geometric construction of spline curves with tension properties," *Computer Aided Geometric Design*, vol. 20, no. 8-9, pp. 579–599, 2003.

[17] Y. Zhu and X. Han, "Curves and surfaces construction based on new basis with exponential functions," *Acta Applicandae Mathematicae*, vol. 129, pp. 183–203, 2014.

[18] P. Costantini, "Curve and surface construction using variable degree polynomial splines," *Computer Aided Geometric Design*, vol. 17, no. 5, pp. 419–446, 2000.

[19] M.-L. Mazure, "Quasi-Chebyshev splines with connection matrices: application to variable degree polynomial splines," *Computer Aided Geometric Design*, vol. 18, no. 3, pp. 287–298, 2001.

[20] M.-L. Mazure, "Blossoms and optimal bases," *Advances in Computational Mathematics*, vol. 20, no. 1-3, pp. 177–203, 2004.

[21] T. Bosner and M. Rogina, "Variable degree polynomial splines are Chebyshev splines," *Advances in Computational Mathematics*, vol. 38, no. 2, pp. 383–400, 2013.

[22] P. Costantini, F. Pelosi, and M. L. Sampoli, "New spline spaces with generalized tension properties," *BIT Numerical Mathematics*, vol. 48, no. 4, pp. 665–688, 2008.

[23] X. Han and Y. Zhu, "Curve construction based on five trigonometric blending functions," *BIT Numerical Mathematics*, vol. 52, no. 4, pp. 953–979, 2012.

[24] M. Hoffmann, I. Juhasz, and G. Karosz, "A control point based curve with two exponential shape parameters," *BIT Numerical Mathematics*, vol. 54, no. 3, pp. 691–710, 2014.

[25] M.-L. Mazure, "On a general new class of quasi Chebyshevian splines," *Numerical Algorithms*, vol. 58, no. 3, pp. 399–438, 2011.

[26] Y. P. Zhu, X. L. Han, and S. G. Liu, "Curve construction based on four $\alpha\beta$-Bernstein-like basis functions," *Journal of Computational and Applied Mathematics*, vol. 273, no. 1, pp. 160–181, 2015.

[27] Y. Zhu and X. Han, "New trigonometric basis possessing exponential shape parameters," *Journal of Computational Mathematics*, vol. 33, no. 6, pp. 642–684, 2015.

[28] P. Costantini, P. D. Kaklis, and C. Manni, "Polynomial cubic splines with tension properties," *Computer Aided Geometric Design*, vol. 27, no. 8, pp. 592–610, 2010.

[29] P. Costantini and C. Manni, "A geometric approach for Hermite subdivision," *Numerische Mathematik*, vol. 115, no. 3, pp. 333–369, 2010.

[30] P. Costantini and C. Manni, "Curve and surface construction using Hermite subdivision schemes," *Journal of Computational and Applied Mathematics*, vol. 233, no. 7, pp. 1660–1673, 2010.

[31] Y.-p. Zhu and X.-l. Han, "New cubic rational basis with tension shape parameters," *Applied Mathematics-A Journal of Chinese Universities Series B*, vol. 30, no. 3, pp. 273–298, 2015.

[32] Q. Duan, F. Bao, S. Du, and E. H. Twizell, "Local control of interpolating rational cubic spline curves," *Computer-Aided Design*, vol. 41, no. 11, pp. 825–829, 2009.

[33] X. Han, "Convexity-preserving piecewise rational quartic interpolation," *SIAM Journal on Numerical Analysis*, vol. 46, no. 2, pp. 920–929, 2008.

[34] J. Cao and G. Wang, "An extension of Bernstein-Bezier surface over the triangular domain," *Progress in Natural Science*, vol. 17, no. 3, pp. 352–357, 2007.

[35] X. Han and Y. Zhu, "A practical method for generating trigonometric polynomial surfaces over triangular domains," *Mediterranean Journal of Mathematics*, vol. 13, no. 2, pp. 841–855, 2016.

[36] Y. Zhu and X. Han, "Quasi-Bernstein-Bezier polynomials over triangular domain with multiple shape parameters," *Applied Mathematics and Computation*, vol. 250, pp. 181–192, 2015.

[37] M.-L. Mazure, "Chebyshev spaces and Bernstein bases," *Constructive Approximation. An International Journal for Approximations and Expansions*, vol. 22, no. 3, pp. 347–363, 2005.

[38] M.-L. Mazure, "On a new criterion to decide whether a spline space can be used for design," *BIT Numerical Mathematics*, vol. 52, no. 4, pp. 1009–1034, 2012.

[39] L. L. Schumaker, *Spline Functions: Basic Theory*, Cambridge University Press, Cambridge, UK, 3rd edition, 2007.

[40] J. M. Carnicer, E. Mainar, and J. M. Peña, "Critical length for design purposes and extended Chebyshev spaces," *Constructive Approximation*, vol. 20, no. 1, pp. 55–71, 2004.

[41] J. M. Carnicer and J. M. Pena, "Total positive bases for shape preserving curve design and optimality of B-splines," *Computer Aided Geometric Design*, vol. 11, no. 6, pp. 633–654, 1994.

[42] J. M. Carnicer and J. M. Pena, "Total positivity and optimal bases," in *Total Positivity And Its Applications (Jaca, 1994)*, vol. 359, pp. 133–155, Kluwer Academic, Dordrecht, the Netherlands, 1996.

[43] M.-L. Mazure, "Which spaces for design?" *Numerische Mathematik*, vol. 110, no. 3, pp. 357–392, 2008.

[44] D. Salomon and F. B. Schneider, *The Computer Graphics Manual*, Springer, New York, NY, USA, 2011.